DETERMINATION OF NUCLEAR REACTOR FLUX DISTRIBUTIONS USING ANALOGUE COMPUTER TECHNIQUES

by

Richard T. Nowak

B. S., University of Toledo
(1953)

Submitted in Partial Fulfillment

of the Requirements for the

Degree of Master of Science

at the

MASSACHUSETTS INSTITUTE OF TECHNOLOGY

January, 1958

Signature of Author: Signature redacted
Department of Chemical Engineering,
January 17, 1958

Certified by: Signature redacted
Thesis Supervisor

Accepted by: . . . .
Chairman,
Departmental Committee on Graduate Thesis

DETERMINATION OF NUCLEAR REACTOR FLUX DISTRIBUTIONS USING ANALOGUE COMPUTER TECHNIQUES

by Richard T. Nowak

Submitted to the Department of Chemical Engineering on January 20 in partial fulfillment of the requirements for the degree of Master of Science.

A proposed design is given for an analog computer to be used for determining the flux distribution in a nuclear reactor under conditions of varying fuel and fission product cross sections. The two-group diffusion equations are solved using the finite difference techniques as applied with an electrical resistor network. The analogy is made that the flow of charge through the network obeys equations similar to those for the flow of neutrons through a reactor.

The computer consists essentially of two resistance networks - one for each of the two-group equations. The resistances used at each junction represent the diffusion and absorption properties of the corresponding spatial volume in the reactor. In the case of the slow group network the absorption properties can be made to vary according to the changes in fuel and fission product cross sections caused by burnup.

Source currents representing the flow of neutrons into each group are provided at the network junction points by an electronic current generator in conjunction with a high speed mechanical scanning switch. The amount of current fed into each point in the slow group network is proportional to the voltage, which represents the neutron flux, on the corresponding spatial point in the fast group network. The reverse applies to the current fed into each point in the fast group network. The proportionality constant between the voltage on the fast network and the current fed into the slow network is determined by the slowing down and resonance absorption properties of the reactor. The proportionality constant between the voltage on a slow network point and the current fed into the corresponding fast network point is determined by the absorption and fission cross sections in the reactor.

An electronic integrator is provided at each slow group network point for the purpose of computing the "flux time" or which is equal to the integral . The output of the integrator is fed into an electronic function generator which determines the changes in the absorption and fission product cross sections. These changes are fed back into the resistance network by changing the proportionality constant between slow network voltages and fast group currents and by controling the variation in the absorption properties of the slow network.

The relationships between the flux time and the absorption and fission cross sections, used in the function generator are determined by solving the set of differential equations describing the changes in properties with flux time. This may be done analytically or by using an analog computer such as the REAC.

Information is read out of the computer in two ways. A fast scanning system of moderate accuracy monitors the voltage on each network point and presents the data on an oscilloscope face. The height of a vertical line represents the magnitude of the voltage while the horizontal position represents the position of the network point. Higher accuracy data is obtainable through the use of a digital voltage applied to one point at a time as required by the operator.

The estimated cost of the computer was based on a unit of one hundred space points. This would include a 100 point fast network, 100 point slow network and all associated equipment. Larger computers could be built up of multiples of this unit. The cost per 100 point unit is estimated at $25,000. This includes all components and fabrication charges. It was felt that this cost was not too high in the light of present computer costs and that such a computer would be a worthwhile addition to a nuclear reactor development facility.

Thesis Supervisor: Dr. T. J. Thompson
Title: Associate Professor of Nuclear Engineering

CONTENTS

I. SUMMARY

A proposed design is given for an analog computer to be used for determining the flux distribution in a nuclear reactor under conditions of varying fuel and fission product cross sections. The two-group diffusion equations are solved using the finite difference techniques as applied with an electrical resistor network. The analogy is made that the flow of charge thru the network obeys equations similar to those for the flow of neutrons through a reactor.

The computer consists essentially of two resistance networks - one for each of the two-group equations. The resistances used at each junction represent the diffusion and absorption properties of the corresponding spatial volume in the reactor. In the case of the slow group network the absorption properties can be made to vary according to the changes in fuel and fission product cross sections caused by burnup.

Source currents representing the flow of neutrons into each group are provided at the network junction points by an electronic current generator in conjunction with a high speed mechanical scanning switch. The amount of current fed into each point in the slow group network is proportional to the voltage, which represents the neutron flux, on the corresponding spatial point in the fast group network. The reverse applies to the current fed into each point in the fast group network. The proportionality constant between the voltage on the fast network and the current fed

into the slow network is determined by the slowing down and resonance absorption properties of the reactor. The proportionality constant between the voltage on a slow network point and the current fed into the corresponding fast network point is determined by the absorption and fission cross sections in the reactor.

An electronic integrator is provided at each slow group network point for the purpose of computing the "flux time" or Θ which is equal to the integral $\Theta = \int_0^t \phi(t)\,dt$. The output of the integrator is fed into an electronic function generator which determines the changes in the absorption and fission product cross sections. These changes are fed back into the resistance network by changing the proportionality constant between slow network voltages and fast group currents and by controling the variation in the absorption properties of the slow network.

The relationships between the flux time and the absorption and fission cross sections, used in the function generator are determined by solving the set of differential equations describing the changes in properties with flux time. This may be done analytically or by using an analog computer such as the REAC.

Information is read out of the computer in two ways. A fast scanning system of moderate accuracy monitors the voltage on each network point and presents the data on an oscilloscope face. The height of a vertical line represents the magnitude of the voltage while the horizontal position represents the position of the network point. Higher accuracy data is obtainable through the use of a digital voltage applied to one point at a time as required by the operator.

The estimated cost of the computer was based on a unit of one hundred space points. This would include a 100 point fast network, 100 point slow network and all associated equipment. Larger computers could be built up of multiples of this unit. The cost per 100 point unit is estimated at $25,000. This includes all components and fabrication charges. It was felt that this cost was not too high in the light of present computer costs and that such a computer would be a worthwhile addition to a nuclear reactor development facility.

II. INTRODUCTION

During the early stages of the design of a nuclear reactor it is often necessary to consider a number of different configurations of the fuel, moderator, reflector and other components in order to produce optimum results in the finished design. One property of the reactor which is important in many of the considerations is the neutron flux distribution in the reactor. This is necessary for computing such things as the magnitude and position of the maximum temperature, the effectiveness of the control rods and the change in fuel concentration due to burnup throughout the reactor. The flux distribution is dependent upon the configuration of the reactor and must be determined for each configuration considered.

The calculation of the neutron flux distribution may be done by a variety of methods. The method chosen will depend on the accuracy required and the time and facilities available to the designer. The use of the one energy group diffusion equation offers the simplest means of setting up a calculation once the macroscopic properties of the reactor are known. Analytic solutions are possible with simple geometries. This method unfortunately is limited to bare reactors as it does not treat control rods and reflectors accurately.

The multi-group diffusion equations offer a means of accounting for the effects of the reflector and control rods. Analytic solutions are possible for simple geometries. Numerical solutions using electronic computers are resorted to in many cases of practical interest where the geometries are complex and the number of energy groups large. Both major types of computers, digital (23) and analog (22), have been used for this work. The digital computer gives answers of high numerical accuracy quickly but at rather high cost. The analog computer - although a specialized machine - produces answers of somewhat less accuracy slower but at lower cost. The compromise must be made, as in many problems involving the two types of machines, between accuracy and cost.

The accuracy attainable in predicting the actual neutron flux distribution with the multi-group calculations does not necessarily increase with the number of energy groups as is indicated in some of the current literature on this subject (2). The calculations are done in sequence using results from the previous calculations as input data for each succeeding calculation. Small errors in the nuclear properties assigned to each energy group due to uncertainties in experimental data can lead to serious errors in the final answer due to error buildup throughout the calculation. These errors will not be numerical as great accuracy is obtainable from the digital machine but will be inherent to the multigroup method. In using a small number of groups the effects of uncertainties in the nuclear properties tend to cancel out because of the large energy groups. It is possible that the two or three group calculations would give more satisfactory results even though they are not quite as rigorous.

The Boltzman neutron transport equation is quite extensively used in making neutron flux distribution calculations. In this type of calculation cognizance is taken of the fact that the diffusion equation is not a true representation of the neutron behavior in the reactive assembly but is an approximation which holds only under specific conditions. The transport equation is a more rigorous representation of the behavior of the neutrons in the reactor but still some approximations are necessary for its use. Often exact solutions are impossible or very difficult and numerical solution methods using digital computers must be used (6).

The Monte Carlo method also makes use of the digital computer. Here the basic operation is not the solution of an equation describing the average behavior of a great many neutrons as in the transport and diffusion equations. The Monte Carlo method consists of following a statistically representative number of neutrons through the details of their lifetimes in the reactor. The events which take place in the life of the neutron are determined by a set of laws governing the phenomena which may take place and by a set of probabilities that govern the occurence of these and other complementary phenomena in the reactive assembly in question.

The Monte Carlo calculation gives very good results if good data on the phenomena taking place in the reactor are available. The set up of the computer however is somewhat tedious and difficult. Because of the nature of the calculation the amount of computer time necessary is fairly large. This makes the calculation expensive.

It is not the purpose of this paper to discuss the merits of each method of calculation mentioned. This would require a great deal more time and space. Rather it should be pointed out that unless the geometry of the reactor is simple enough so that an exact analytic solution to the transport or diffusion equations is possible recourse must be made to the use of computing machinery. The digital machine has great flexibility and may be used with any of the methods mentioned. Excellent results are attainable if the computer is used properly. However the digital machine is large and expensive to operate which precludes its use on many problems which are important but do not merit the necessary large outlay of money.

Analog computer techniques offer the possibility of a lower cost installation with some loss of accuracy and flexibility. In neutron flux distribution problems their use is limited to solving the diffusion equation. Problems with complex geometry and in some cases time dependency may be solved fairly accurately. The value of an analog computer for this type of work will be determined by the validity of the multigroup diffusion equations as applied to the problem under consideration.

A design study was undertaken to investigate the feasibility of building an analog computer system for use in determining reactor flux distributions. In the course of the preliminary investigation of the computer system it appeared that a simulator might be designed which would permit the determination of the flux distribution in a reactor under conditions of variable nuclear properties due to fuel depletion and fission-product production. The scope of the work was enlarged to include this possibility.

The method of approach to the problem was to develop the analogy between the diffusion of neutrons through the reactor and the diffusion of charge through an electrical network. Once the analogy was established the requirements of the electrical apparatus necessary for the operation of the network were determined. To fill these requirements commercially available equipment was designated where applicable and where no such equipment was available it was designed. No attempt was made to construct the system as funds were not available.

III. NETWORK DEVELOPMENT

A. CORE

The simplest set of equations which provide fairly good results for reflected reactors are the two-group diffusion equations. The method proposed for the solution of these equations is the use of finite difference techniques as applied with a network of resistors used to simulate the nuclear properties of the reactor. The use of resistor networks for this purpose has been carried on by various experimenters (7)(8)(9) and some work has been done in applying networks of passive elements to partial differential equations other than the diffusion equation (18). The network analogy presented here is similar to that of Harrer (7).

The two-group equations for the reactor core are

(1) $D_f \nabla^2 \phi_f - \Sigma_{af}\phi_f + \eta \epsilon f \Sigma_{as} \phi_s = 0$

(2) $D_s \nabla^2 \phi_s - \Sigma_{as}\phi_s + p \Sigma_{af} \phi_f = 0$

Subscript f refers to the "fast" or high energy group and s refers to the "slow" or thermal energy group. Σ_a is the macroscopic removal cross section which in the case of the fast group represents removal from the group by slowing down. All real absorption in the fast group is assumed to be lumped as an escape probability (p) at the boundary between the fast and slow groups. Thus the source term for the slow group is $p\Sigma_{af}\phi_f$ instead of $\Sigma_{af}\phi_f$ alone. The source term for the fast group is $\eta\epsilon f\Sigma_{as}\phi_s$ which is the number of neutrons produced in the fast group per cubic centimeter from the thermal flux ϕ_s. A more complete development of the two group equations is given by Glasstone and Edlund (5).

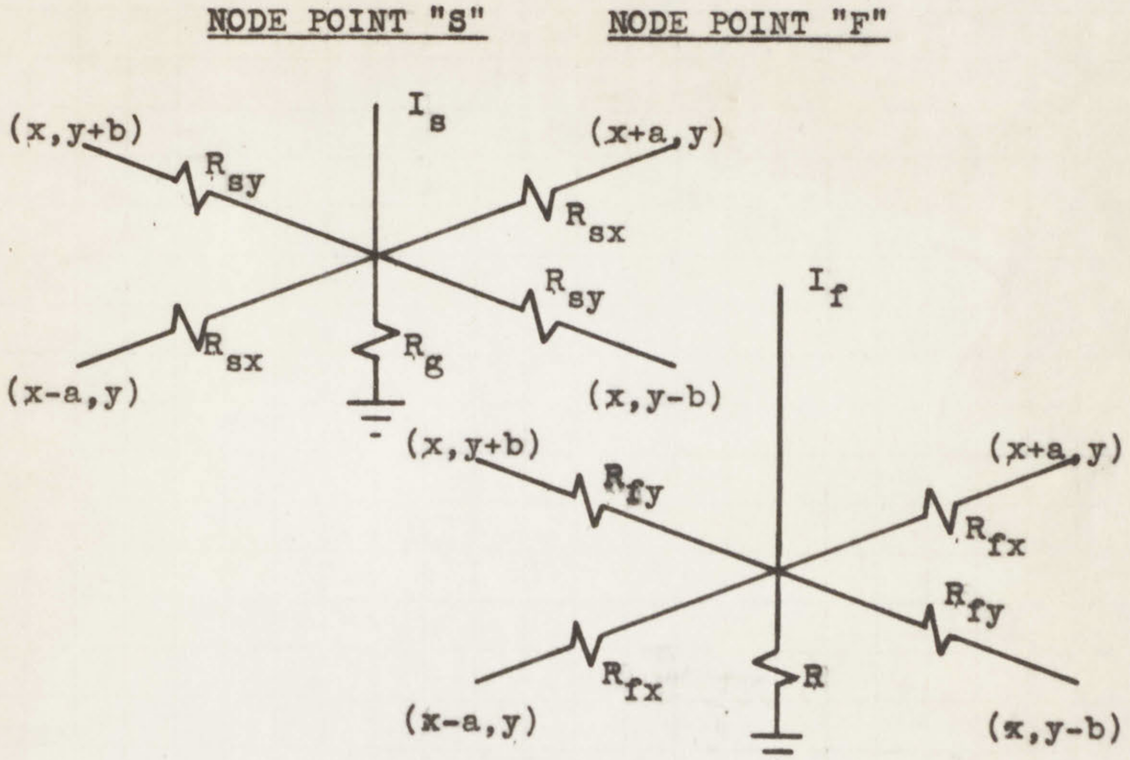

FIGURE 1

Consider a pair of resistor networks made up of a number of the representative junction points illustrated in figure 1. A balance for the currents at the node point "F" located at the spatial position (x,y) may be written as

(3)

$$\frac{V_{f(x+a,y)}-V_{f(x,y)}}{R_{fx}}+\frac{V_{f(x-a,y)}-V_{f(x,y)}}{R_{fx}}+I_{f(x,y)}+$$

$$\frac{V_{f(x,y-b)}-V_{f(x,y)}}{R_{fy}}+\frac{V_{f(x,y+b)}-V_{f(x,y)}}{R_{fy}}-\frac{V_{f(x,y)}}{R_{\gamma}}=0$$

A Taylor series expansion of $V_f(x,y)$ about the point (x,y) is

(4) $V_f(x+a,y) = V_f(x,y) + \frac{a}{1!}\frac{\partial V_f(x,y)}{d x} + \frac{a^2}{2!}\frac{\partial^2 V_f(x,y)}{\partial x^2} + \ldots.$

(5) $V_f(x-a,y) = V_f(x,y) - \frac{a}{1!}\frac{\partial V_f(x,y)}{\partial x} + \frac{a^2}{2!}\frac{\partial^2 V_f(x,y)}{\partial x^2} + \ldots.$

(6) $V_f(x,y-b) = V_f(x,y) - \frac{b}{1!}\frac{\partial V_f(x,y)}{\partial y} + \frac{b^2}{2!}\frac{\partial^2 V_f(x,y)}{\partial y^2} + \ldots.$

(7) $V_f(x,y+b) = V_f(x,y) + \frac{b}{1!}\frac{\partial V_f(x,y)}{\partial y} + \frac{b^2}{2!}\frac{\partial^2 V_f(x,y)}{\partial y^2} + \ldots.$

Equations 4, 5, 6, 7 are substituted into 3 with the following results if derivatives higher than the second are neglected.

(8) $\frac{a^2}{R_{fx}}\frac{\partial^2 V_f(x,y)}{\partial x^2} + \frac{b^2}{R_{fy}}\frac{\partial^2 V_f(x.y)}{\partial y^2} - \frac{V_f(x,y)}{R_\gamma} + I_f = 0$

$\frac{a^2}{R_{fx}} = \frac{b^2}{R_{fy}}$ as isotropic properties are required.

$$\frac{a^2}{R_{fx}}\left[\frac{\partial^2 V_f(x,y)}{\partial x^2} + \frac{\partial^2 V_f(x,y)}{\partial y^2}\right] - \frac{V_f(x,y)}{R_\gamma} + I_f = 0$$

(9) $\frac{a^2}{R_{fx}}\nabla^2 V_{f(x,y)} - \frac{V_f(x,y)}{R_\gamma} + I_f = 0$

Only two dimensions have been considered here but it is apparent that the results would be identical for a three dimensional network. Equation (9) would result with $\nabla^2 = \left[\frac{\partial^2}{\partial x^2} + \frac{\partial^2}{\partial y^2} + \frac{\partial^2}{\partial z^2}\right]$

A similar expansion may be carried out on the point "S"(x,y) with the following result.

(10) $\frac{a^2}{R_{sx}}\nabla^2 V_s(x,y) - \frac{V_s(x,y)}{R_g} + I_s = 0$

If $I_s = A_1 V_f(x,y)$ and $I_f = A_2 V_s(x,y)$ where A_1 & A_2 are arbitrary constants are substituted into equations (9) and (10) and the resulting equations compared with equations (1) and (2) the similarity between the equations is apparent. An analogy may be set up as follows

(11)

$$\phi_f - V_f \qquad D_s - \frac{a^2}{R_{sx}} \qquad A_2 - \eta\epsilon f \Sigma_{as}$$

$$\phi_s - V_s \qquad \Sigma_{af} - \frac{1}{R_\gamma} \qquad A_1 - p\Sigma_{af}$$

$$D_f - \frac{a^2}{R_{fx}} \qquad \Sigma_{as} - \frac{1}{R_g}$$

Also by manipulation

$$\frac{\Sigma_{as}}{D_s} = \frac{1}{L^2} = \frac{R_{sx}}{a^2 R_g} \qquad \frac{\Sigma_{af}}{D_f} = \frac{1}{T} = \frac{R_{fx}}{a^2 R_\gamma}$$

where T = fermi age and L = Diffusion Length

The currents flowing in the networks of figure 1 have the following correspondence. The currents flowing in the "diffusion" resistors R_s and R_f correspond to the neutrons diffusing thru the spatial volume about point (x,y) . The current in R_γ represents the current of neutrons slowing down out of the fast group in the same volume. The current in R_g represents the current of absorbed neutrons. The current I_f represents the neutrons born in the space about (x,y) by fission and I_s represents the neutrons slowing down into the thermal energy group.

From this set of equations using a proper scale factor between the equations in V and ϕ a pair of networks can be constructed which will provide solutions for the two group equations. The currents I_s and I_f required by the networks are obtained as shown in figure (2). The node points S(x,y) and F(x,y) are connected through the current generators whose output current is proportional to the input voltage. The proportionality constants A_1 and A_2 are determined by the properties of the reactive assembly as given in equations (11).

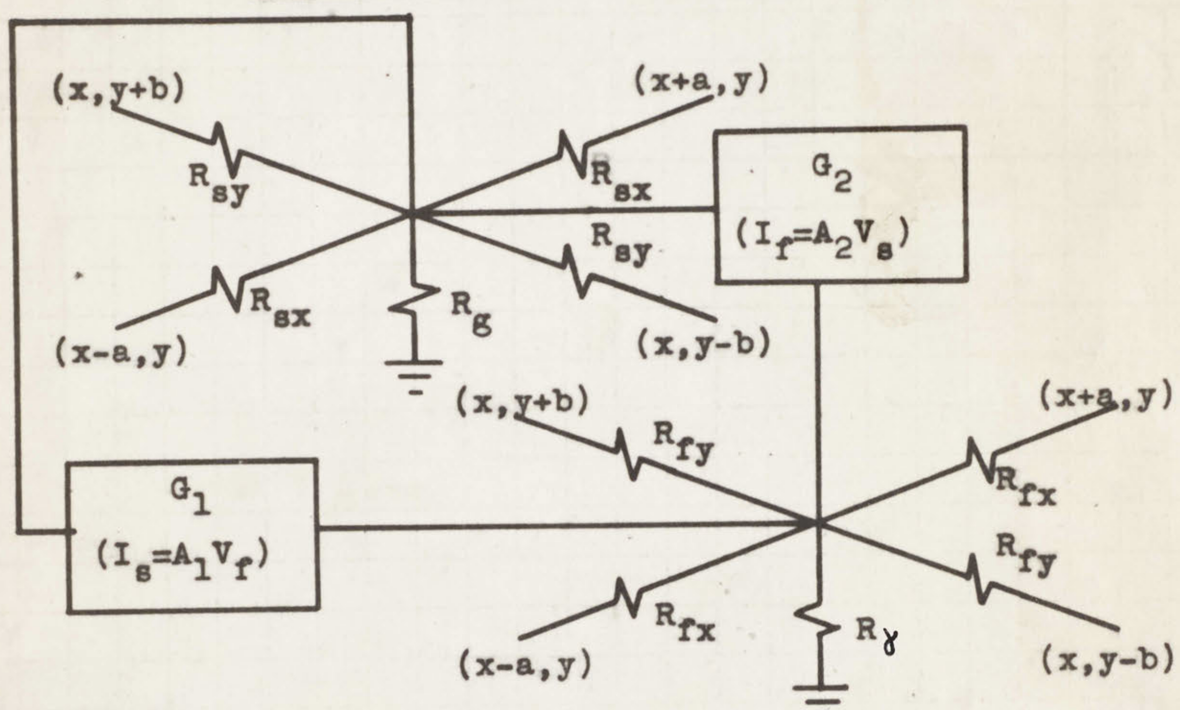

FIGURE 2

B. REFLECTOR

The two group equations applied to the reflector of the reactor as given by Glasstone and Edlund are

$$(12) \quad D_f \nabla^2 \Phi_f - \Sigma_{af} \Phi_f = 0$$

$$(13) \quad D_s \nabla^2 \Phi_s - \Sigma_{as} \Phi_s + p \Sigma_{af} \Phi_f = 0$$

The nomenclature used is the same as above. The values of the constants D_f, Σ_{as} etc. are now determined by the properties of the reflector. The same scale factors are used for computing the constants for the reflector as were used for the core. The only difference between the two sets of equations is that no multiplication or source term is present for the fast group. The same type of resistor network is used for the reflector as was used for the core with the exception that the generator G_2 is removed because there is no source term for the fast group. This is illustrated in figure 3.

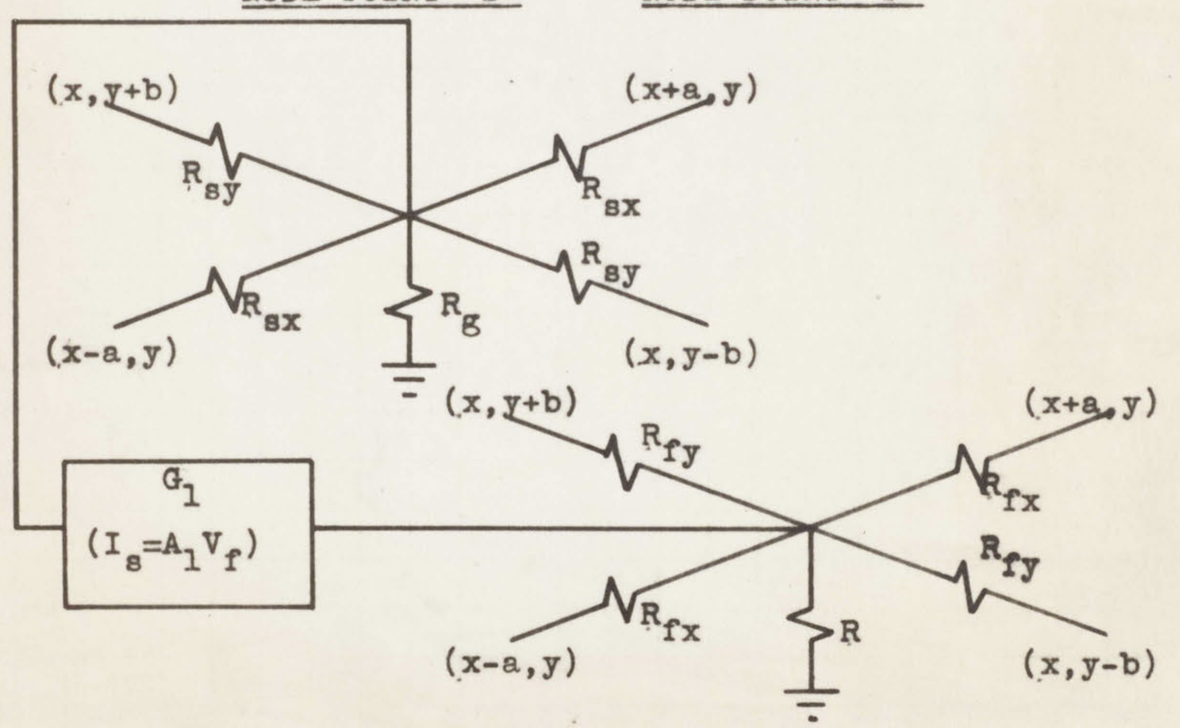

FIGURE 3

III. NETWORK DEVELOPMENT (CONT.)

C. BOUNDARY CONDITIONS

There are two boundary conditions used in solving the diffusion equations which must be treated properly by the resistor network. These are that the flux must be zero for both the fast and slow energy groups at the external boundary of the reactive assembly and that the flux for both groups must be continuous across the boundaries between different regions inside the assembly. The first condition is met by grounding each network at the outer boundary.

The second condition is met by constructing a network for each region of the reactor and joining these networks at the interface between the two regions. The same grid is used for all regions. This is illustrated in figures (4) and (5). Figures (4) and (5) show the core and reflector regions of a portion of a cylindrical reactor laid out in a network of lines representing the resistors in the simulator.

There are two methods of treating the interface between the two regions. One is to approximate the actual boundary by a series of straight lines along or midway between the lines of the network. This is illustrated in figure (4). The portion of the network inside the boundary is constructed using the properties of that region and the two networks are joined together at the boundary.

If the interface occurs midway between the node points the values of the diffusion resistors perpendicular to the interface require adjustment according to the equation

$$R\ (\text{interface}) = R/2\ (\text{core}) + R/2\ (\text{reflector})$$

The absorption resistances Rg and R and the diffusion resistances parallel to the interface need not be adjusted.

If the interface occurs at the node point the diffusion resistances perpendicular to the interface are not adjusted. The absorption and the diffusion resistances along the interface require adjustment according to the equation

$$R\ (\text{interface}) = \frac{2R\ (\text{core})\quad R\ (\text{reflector})}{R\ (\text{core}) + R\ (\text{reflector})}$$

The second method of treating the interface is to approximate it with a series of straight lines connecting the intersections of the actual interface and the grid lines of the resistor network as shown in figure (5). As before, the networks inside and outside the interface are constructed using resistances determined by the properties of the two regions. The resistances adjacent to and crossing the interface are adjusted according to the equations

$$R_{fx} = aR_{fx}\ (\text{core}) + (1-a)R_{fx}\ (\text{reflector})$$

$$R_{fy} = bR_{fy}\ (\text{core}) + (1-b)R_{fy}\ (\text{reflector})$$

$$R_g = \frac{R_g\ (\text{core})\quad R_g\ (\text{reflector})}{AR_g\ (\text{core}) + BR_g\ (\text{reflector})}$$

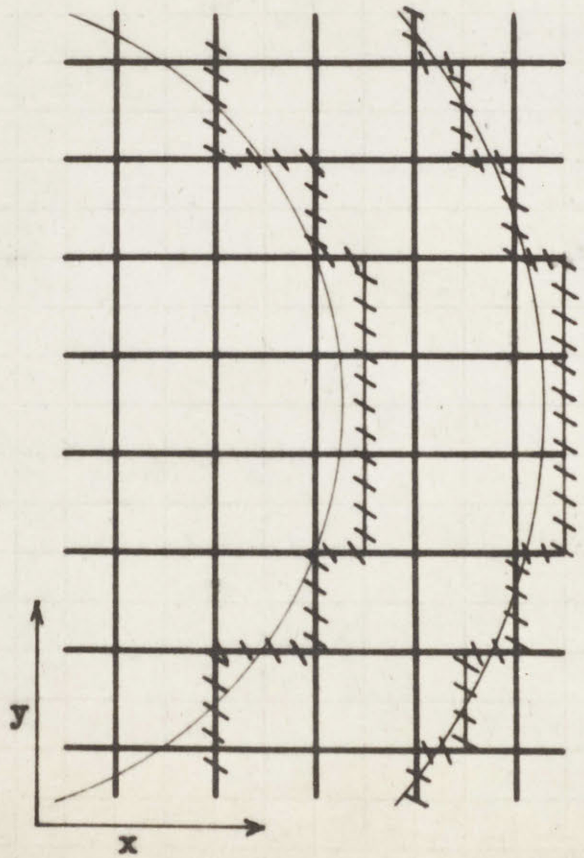

FIGURE 4.

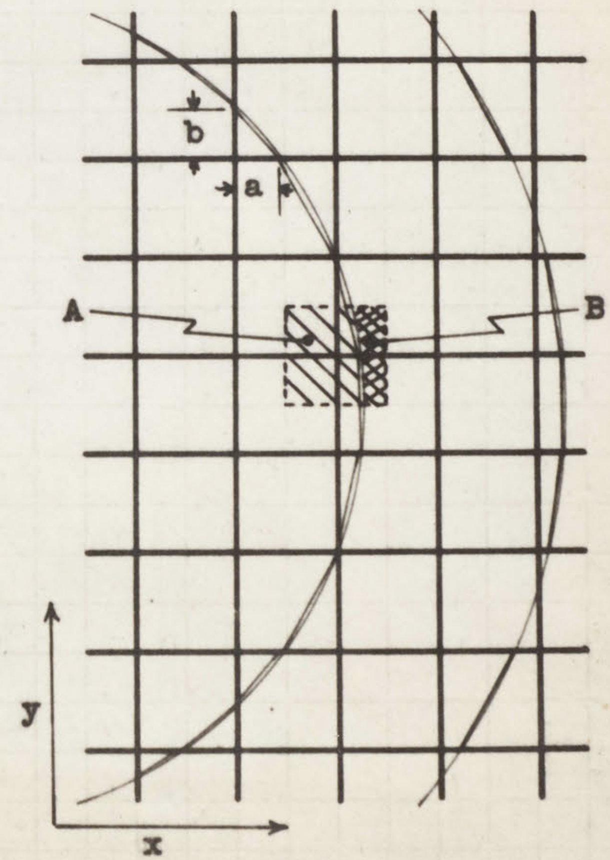

FIGURE 5.

The constants a and b are the fractions of the unit cell distance from the node point to point of intersection of the interface with the grid lines as illustrated in figure (5). The constants A and B are the fractions of the area of the unit cell about the node point occupied by the core and reflector respectively as shown in figure (5).

D. SOURCES

As with most finite difference techniques the accuracy of the solution will depend on the separation between nodes. The results will improve as the spacing between nodes is decreased. This requires that networks with large numbers of nodes be used in order to represent a reactor of any size.

The major difficulty in building large networks of this type is supplying the source current required at each network point. Various schemes have been devised for providing these source currents (11)(7)(8)(9).

The system proposed here is developed on ideas put forth by Harrer (7). Instead of having a separate current feed circuit at each spatial node point the points are connected sequentially through a scanning switch (SW) to an amplifier (A) shown in figure 6 which supplies a current (I) at its output proportional to the input voltage (V). The proportionality constant (a) and the resistances are determined by the properties of the reactive assembly being simulated. A capacitance (C) of large value is connected at each point to provide current to the net point during the "off" period in the switching sequence. The size of the capacitor is chosen large enough so the variation in voltage due to discharge is small ie 1/2 - 1%. The capacitor is kept charged to the proper voltage by the current supplied from the amplifier during the "on" period. In this way the capacitor acts as a constant current source for the network.

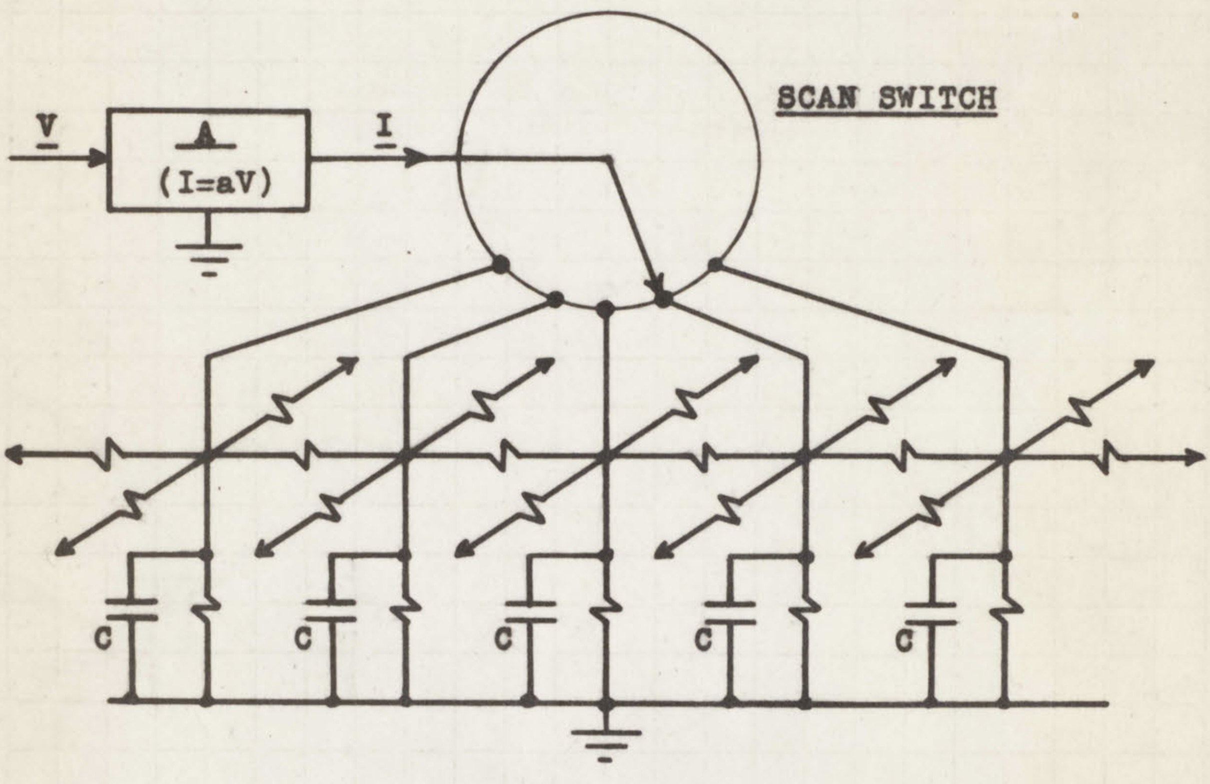

FIGURE 6.

E. SYSTEM FOR DETERMINATION OF STEADY STATE FLUX DISTRIBUTION

The system for the determination of the steady state flux distribution consists of a fast flux resistor network, a slow flux resistor network and the electronic apparatus necessary to supply source currents at the node points.

Figure 7 shows a block diagram of the system set up to simulate one quarter of a circular slab section taken from a cylindrical reactor. A network of one hundred points is used for each energy group. Each junction is identical with the detailed junction for the respective region except for those at the boundary between reflector and core. The resistance values used are computed using equations (11) and the scale factors discussed in Appendix B. The resistances immediately adjacent to or crossing the boundary are computed using the equations from the section on boundary conditions.

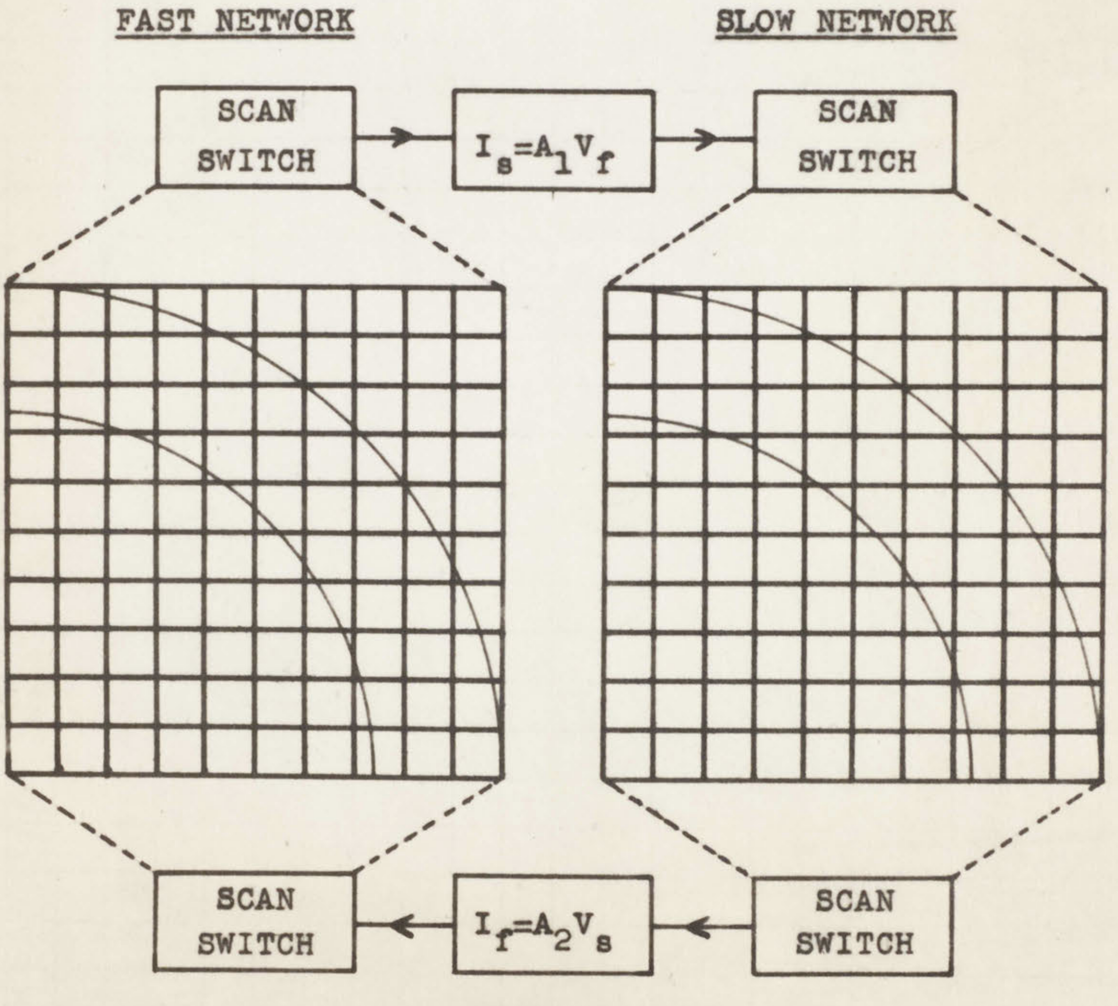

FIGURE 7.

The electronic apparatus consists of two current generators as described in Section IV and a high impedance voltmeter for taking measurements.

After the system is set up the scanning switches and current generators are activated. The gain of the current generators is set rather high so the voltages will build up on the network quickly. It may be necessary to have an extra source of current to put the circuit into operation. Measurements of the network voltages are taken at various points in the net. When the maximum network voltage nears the maximum voltage allowed by the electronic apparatus, the gain of the generators is reduced.

The gain of the generator used to supply the slow network is adjusted to the value computed from equations (11). The gain of the generator used to supply the fast network is adjusted until a steady state condition is reached on both networks with no voltages exceeding the maximum allowed by the components of the current generators. The multiplication factor of the reactor can then be computed from this gain and the properties of the reactor.

F. CIRCUIT FOR NON-CONSTANT PROPERTIES

The problem of using the system described previously for the determination of flux distributions under conditions of non-constant properties is now considered. The discussion is limited to the effects of the long term property changes caused by fission-product buildup and fuel burnup and fission product production. The reactor will be considered critical at all times.

In a small representative volume element of the core of a fixed fuel reactor the concentration of fuel, fission products, moderator and other constituents of the core change with time due to the fission, capture and other processes taking place. The extent of the change in each constituent depends on the type of reactor, the power level and other conditions unique to the reactor in question.

In order to have some idea of the changes involved, a reactor using a U^{238}-U^{235} fuel in a homogeneous core was taken as a sample problem and the concentration changes calculated. The work is described in Appendix A. The equations used were taken from the notes on the forth-coming book by Benedict and Pigford, Chapter 3. The analytic solutions to the differential equations describing the system under consideration are given but are rather involved for graphical presentation. Therefore the equations were set up on the REAC in the servo-mechanisms laboratory and solutions run off. Some representative recordings are given in Appendix A. The major changes are in Σ_{as} and $\eta \epsilon f \Sigma_{as}$.

The change in Σ_{as} is due mainly to the production of fission products with cross sections different from the fuel cross section and to the change in concentration of the high cross section fuel. The change in $\eta \epsilon f \Sigma_{as}$ is due to a change in $\eta \epsilon f$ caused by a change in the type of fuel from pure U^{235} to a U^{235} Pu^{239} Pu^{241} mixture and by the change in Σ_{as}.

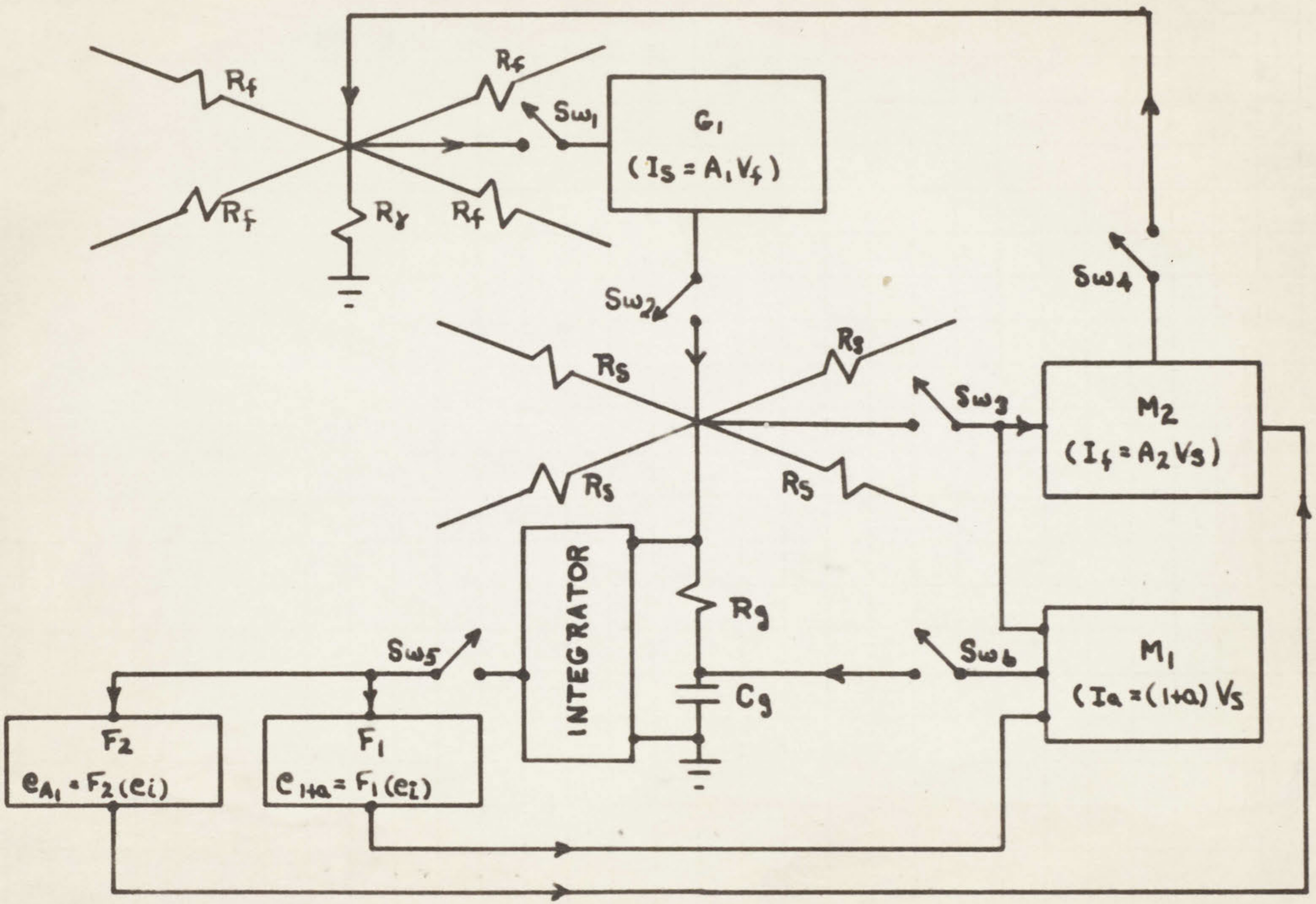

Rf
Rf
Rf
Rf
Rr
Sw1
G1
(Is = A1Vf)
Sw2
Sw3
Sw4
Rs
Rs
Rs
Rs
M2
(If = A2Vs)
INTEGRATOR
Rg
Cg
Sw5
Sw6
M1
(Ia = (1+a) Vs
F2
eA1 = F2(ei)
F1
e1+a = F1(ei)

FIGURE 8.

The problem at this point is one of finding a means of applying the information on the fuel burnup and fission product production to the two group network developed in the previous sections. This can be done using the circuit shown in figure 8. In this figure M_1 and M_2 are current amplifiers whose output current is proportional to the input voltage. The proportionality factors A_2 and $1+a$ are controlled by voltages from the associated function generators F_1 and F_2. The input to the function generators is the signal from the integrator S connected to the net point (x,y).

The network is assumed to be operating with a steady-state flux distribution characteristic of the clean reactor with the integrators initially set at zero signal. The integrator is then connected and generates a signal representing the integral of the flux with respect to time or the flux time T. This signal is fed into the function generator F_2 which generates a signal representing change in fuel cross section and type with flux time. The functions describing the variation of properties with flux-time are arrived at by methods described in Appendix A. This change in fuel cross-section and type changes the proportionality factor A_2 between the slow flux and the fission neutrons produced. The change in proportionality is accomplished by feeding the output from F_2 into M_2. In this way the changes in $\eta \epsilon f \Sigma_{as}$ with flux time can be represented.

The circuit involving M_1 and F_1 operates as follows. It has been previously shown in equations (11) that an analogy exists between Σ_{as} and $\frac{1}{R_g}$. A variation in Σ_{as} requires a variation in $\frac{1}{R_g}$. This may be accomplished with a circuit as shown in figure 9.

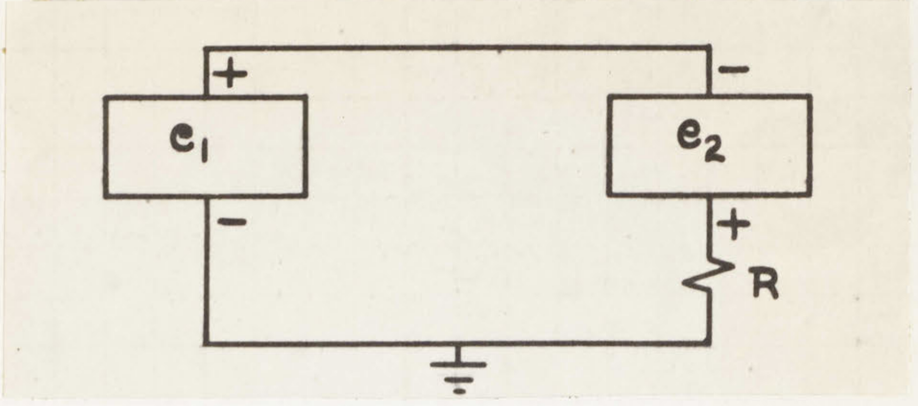

FIGURE 9.

The current through the resistance R is given by $i = \frac{e_1+e_2}{R}$. The voltage e_2 is controlled to be $e_2 = ae_1$. The expression for the current then becomes $i = \frac{e_1+ae_1}{R} = \frac{e_1(1+a)}{R}$. The conductance of the circuit as seen from e_1 is then $\frac{1}{R} = \frac{1+a}{R}$.

This development may be applied to the circuit of figure 8 if e_1 is replaced by V_s, e_2 by M_1 and R by R_g. The factor a is provided by the function generator F_1 which is fed by the signal from the integrator. The effect on the resistor network is the conductance at the point (x,y) is changed simulating a change in Σ_{as} the absorption cross section in the slow group. The degree of change is determined by the fission product buildup as given by the equations in Appendix A.

In order that a complete computing combination is not required at each network point large capacitors are used at the points of current feed as was done for the source currents. Each point is then operated on sequentially through a scanning switch as shown in figure 8. Integration is provided by the integrator I the details of which are given in the section on circuit details.

To deal with the "real" multiplication factor of the reactor when it is simulated provision must be made for the change in absorption cross section caused by control rod motion. A practical reactor is designed with some excess reactivity in its cold clean state in order to provide a usable life for the reactor. This excess reactivity is absorbed by the control rods early in the life of the fuel loading and is used up as the fuel burns up and fission products accumulate. When the excess reactivity drops to zero or slightly below the reactor becomes sub-critical and operation ceases. If the clean reactor is simulated and the clean properties are used in the analogies with no scaling changes the simulator will be "super-critical" unless "control rods" are provided.

According to Harrer (7) the simulator contemplated here will react analogously to the real reactor as regards its kinetic behavior.

If the total input of current to the network by the amplifiers A_1 and M_1 is larger than the total current which flows out of the network through the R_g's and which leaks out at the boundaries of the network the amount of charge in the system will increase and the voltages on the storage condensers will increase. Likewise if the total input current is less than the total output current the voltages will decrease. If the properties of the simulator are scaled properly to the properties of the reactor the only way to provide control over the current balance in the network is by simulating the control rods of the reactor. The control rods may be simulated as "black" by grounding the points in the slow network in the area occupied by the rod. "Gray" rods may be simulated by inserting fixed resistors of the proper values at the net points involved. No current feed is provided to the fast network over the points occupied by the control rod as there would be no multiplication in this region. These points would not be grounded however. In the case of "black" control rods no current feed is provided to the slow network in the rod areas. For "grey" rods the amount of feed is reduced depending on the properties of the rods. The simulation of the "grey" rods will be discussed further under CONTROL ROD SIMULATION.

IV. DESCRIPTION OF PROPOSED REACTOR SIMULATOR

A block diagram of the system proposed for the determination of nuclear reactor flux distributions under conditions of non-constant properties is given in figure 9a. The system consists of the fast and slow group networks described previously along with a control-rod simulator and recording and measuring instruments.

A. NETWORKS

A suggested layout for the network panels is given in figure 10. The choice of a unit cell 6 in. high by 4 in. wide was chosen in order to provide enough space behind each unit for the integrator and capacitors required. The layout of a unit cell is shown in detail in figure 11.

The diffusion and absorption resistances are provided by dual unit concentric shaft potentiometers. The two potentiometers, one of 5 megohms, the other of 100 kilohms, are wired in series. The 100 kilohm potentiometer provides a fine adjustment for setting the desired resistance. Logarithmic tapers are specified in order to provide the same percentage error in resistance per unit of rotation for all settings of the potentiometers.

The terminal posts J_1 and J_2 and the switch SW_1 provide access to each potentiometer pair separately for making adjustments. A detailed wiring diagram of the switch plate is shown in the insert in figure 11. Terminal post J_1 provides access to the diffusion resistances and to one

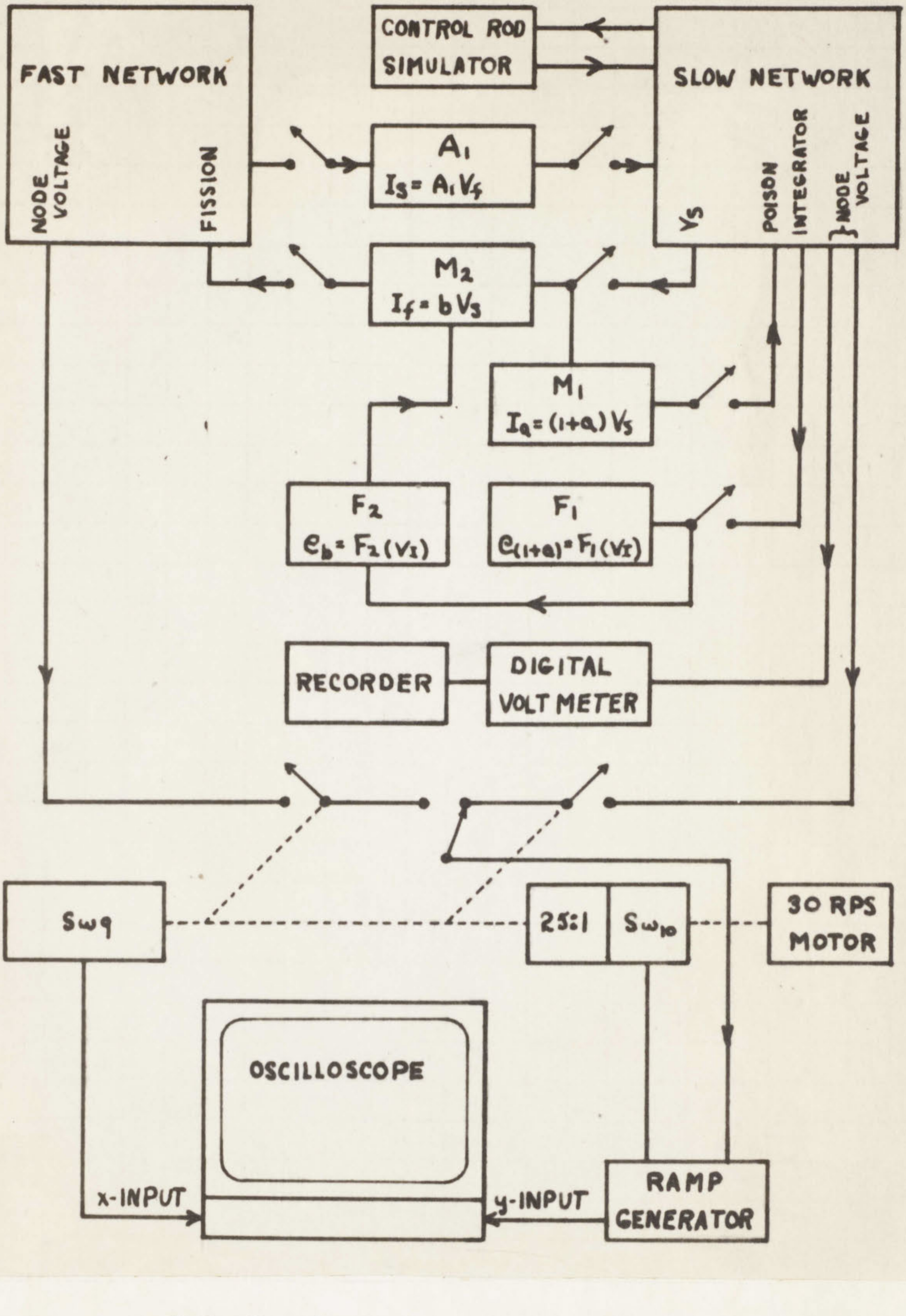
FAST NETWORK
NODE VOLTAGE
FISSION
CONTROL ROD SIMULATOR
SLOW NETWORK
VS
POISON
INTEGRATOR
NODE VOLTAGE
A1
IS = A1 Vf
M2
If = b VS
M1
Ia = (1+a) VS
F2
eb = F2 (VI)
F1
e(1+a) = F1 (VI)
RECORDER
DIGITAL VOLT METER
Sw9
25:1
Sw10
30 RPS MOTOR
OSCILLOSCOPE
x-INPUT
y-INPUT
RAMP GENERATOR

FIGURE 9a

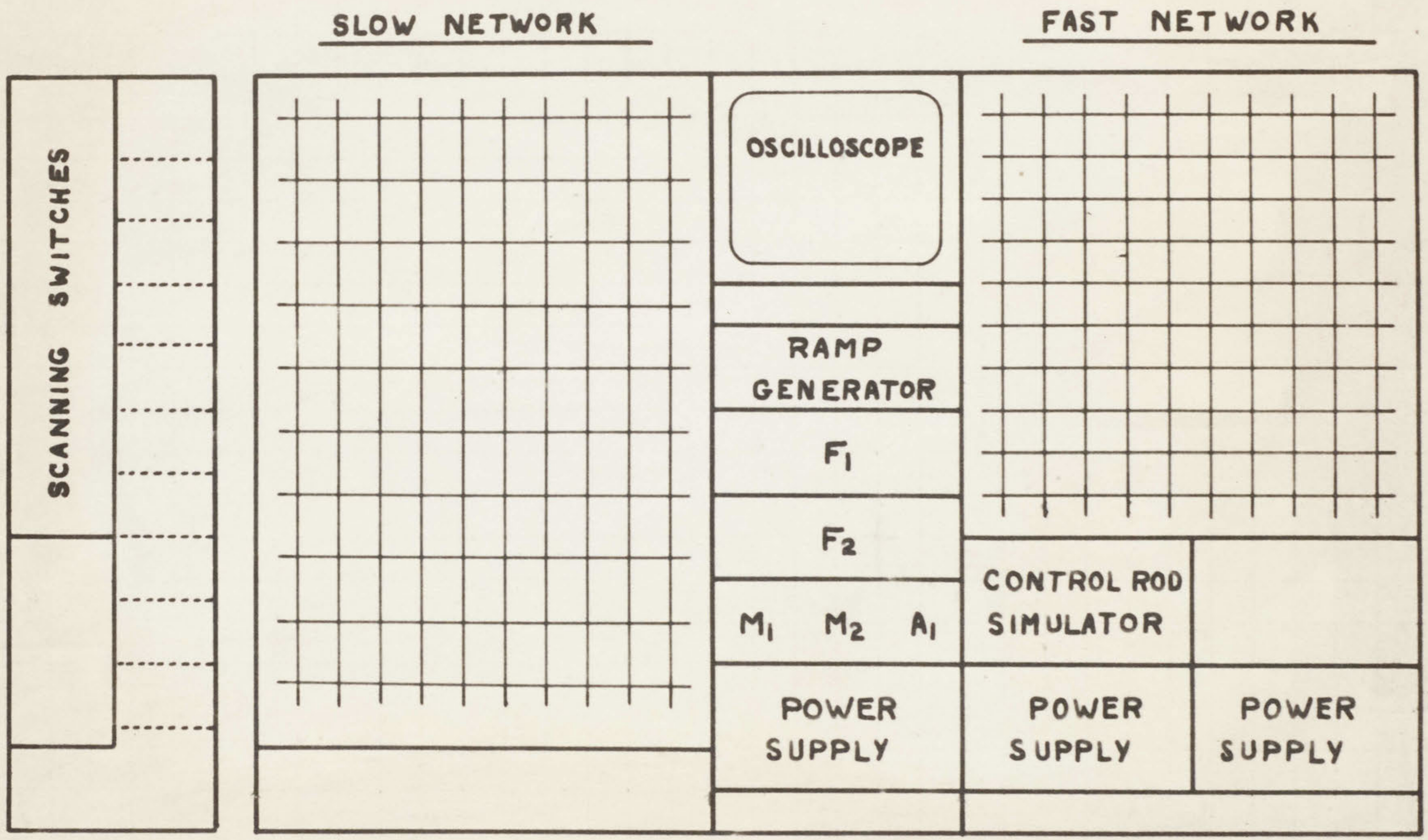
SLOW NETWORK
FAST NETWORK
SCANNING SWITCHES
OSCILLOSCOPE
RAMP GENERATOR
F_1
F_2
M_1 M_2 A_1
CONTROL ROD SIMULATOR
POWER SUPPLY
POWER SUPPLY
POWER SUPPLY

FIGURE 10.

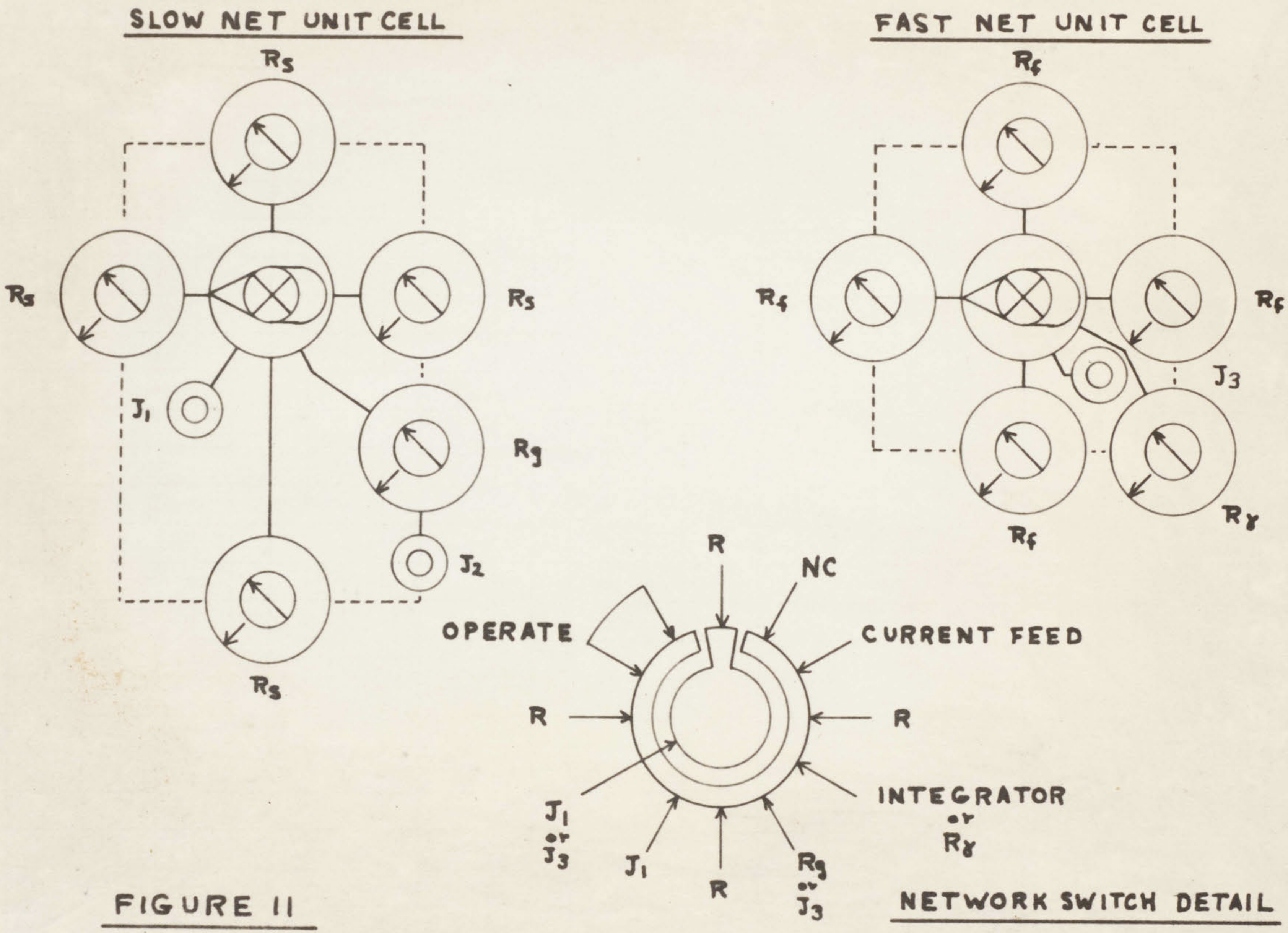

SLOW NET UNIT CELL
R_s
R_s
R_s
R_s
J_1
R_g
J_2
FAST NET UNIT CELL
R_f
R_f
R_f
J_3
R_f
R_γ
R
NC
OPERATE
CURRENT FEED
R
R
INTEGRATOR or R_γ
J_1 or J_3
J_1
R
R_g or J_3
NETWORK SWITCH DETAIL

FIGURE 11

terminal of the absorption resistance. Terminal post J_2 provides access to the other terminal of the absorption resistor, and may be used to short out the absorption feedback capacitor in steady-state problems. One position is provided on the switch for connecting the terminal J_1 directly to the current feed circuits, by passing the potentiometers. This provides for the use of external diffusion and absorption resistances. These could connect directly to the J_1 terminals or could be mounted on boards provided with jacks to plug into the terminals. Thus resistances would not be limited to those provided by the internal potentiometers. Also this would provide a means for connecting the "control rod" absorption resistances at the proper points in the network.

B. SCANNING FREQUENCY

In deciding the scanning frequency of the simulator the following considerations were used. The maximum number of points which can be scanned with a commercially available switch is approximately one hundred. The variation in the voltage on the source condensers in the resistor network should not be greater than one percent and preferably less. The voltage on this condenser will follow a variation represented by $e = e_o \, Exp(-t/RC)$ where e_o is the voltage at the beginning of the discharge, t is the time after the beginning of the discharge, R is the effective resistance of the circuit as seen from the point (x, y) and C is the capacity of the condenser. The error in the voltage will be the difference between e_o and e over one cycle which will be $e_o - e = e_o \left[1-\mathrm{Exp}(-t_o/RC)\right]$ where t_o is the period of the cycle. This may be approximated for small values of t_o by $e_o - e = e_o(t_o/RC)$. For an error of one-half percent $(e_o-e)/e_o = t_o/RC=0.005$. Then $RC = 200t_o$, $t_o = RC/200$ and $f_o = 1/t_o = 200/RC$.

The maximum current supplied by the components used in the current amplifiers is of the order of 10 milliamperes. In order to use currents of this order from the amplifiers it is necessary to have effective resistances of the order of 1 megohm in the network. This value of resistance coupled with a capacitance of approximately 5 microfarads gives an RC time constant of approximately 5 seconds. Then $t_o = 5/200 = 0.025$ second and $f_o = 40$ cps. The current amplifiers at this scanning rate would have to make four thousand computations per second.

C. NETWORK SCANNING SWITCHES

The scanning switches proposed for use with the networks are of the rotary mercury jet type manufactured by Norwood Controls Corp.   . Correspondence with the manufacturer indicates that switches of 100 points per switch and speeds of 200 revolutions per second are available in stock items. Correspondence with manufacturers of the solid contact type switch such as made by Applied Science Corporation of Priceton indicate that the maximum recommended operating speed of this type switch is approximately 900 contacts per second. At 100 contacts per switch this would give 9 rps.

The lifetime of the mercury switch is approximately 1000 hours at maximum speed as compared to 100 hours for the solid switch at the maximum speed quoted above. The solid switches as yet are not available in 100 contact sizes for the condition of break-before-make operation which is required here.

D. CURRENT AMPLIFIERS

The current amplifiers represented by M_1 and M_2 are build of computer components manufactured by George A. Philbrick Researches, Inc. The requirement of computing speed practically limits the choice of components to those manufactured by this company. The maximum frequency response of operational amplifiers currently on the market is in the vicinity of 5000 cps. except for the Philbrick amplifiers with maximum frequencies of 250 KC/s. The proposed operating speed for the simulator amplifiers is 4000 computations per second. In order to reproduce accurately the signal into it, an amplifier should be able to respond to the 100th harmonic of the input frequency. The closest this requirement can be approached here is to use the Philbrick equipment capable of responding to the 60th harmonic.

The current amplifiers may be broken down into two sub-units; the multiplier and the current generator as shown by the block diagram in figure 12. The inputs are shown for current amplifier M_1. The multiplier output is the product of the voltage V_s from the resistor network and voltage $(1 + a)$ from F_2. This is the input to the current generator which produces a current $i = V_s\ (1+a)B$ where B is determined by the scaling involved in the computation.

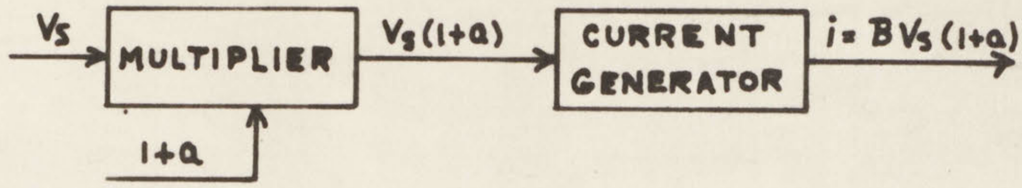

FIGURE 12.

The multiplier is available as a stock item. The proposal is to use the model MU/DV by George A. Philbrick Researches, Inc. (The products of the Philbrick Company will be referred henceforth as GAP/R Model···· as in the literature.)

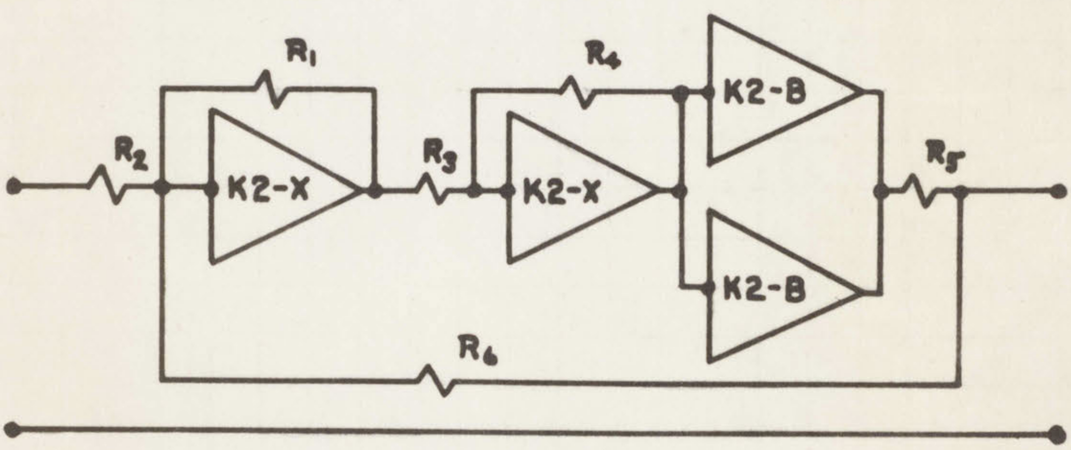

FIGURE 13.

In searching for a commercially built current generator, it was found that none was available. The next best thing was to design one using commercially available components. This was done using Philbrick components in a "bootstrap" type circuit similar to that described by Puckle (19).

A current generator is a device which produces, in accord with some input demand, a current at its output which does not vary with output voltage or impedance. A discussion of current generators may be found in Elmore and Sands (4). A circuit appears in figure 13 which meets the requirements of the current generator as given above. An analysis of the circuit appears in Appendix B.

The operating range of the current generator is limited by the operational amplifiers to a maximum current of 20 ma. at $\pm$ 55V. This places a limit on the voltage which may be used on the network and is the reason for choosing a network current of 10 ma in the section on scanning frequency.

A check was made on the analysis of the current generator by setting up the circuit using the Reeves Analog Computer in the Servo Mechanisms Laboratory. Data were taken of the load voltage versus load resistance at various input voltages. Plots of these data are given in figure 14. These show essentially that the load current i_L remained constant with the input voltage e_o under conditions of varying load resistance. The prime concern was for the stability of the circuit because of the positive feedback involved. No instability or tendency toward instability was noticed.

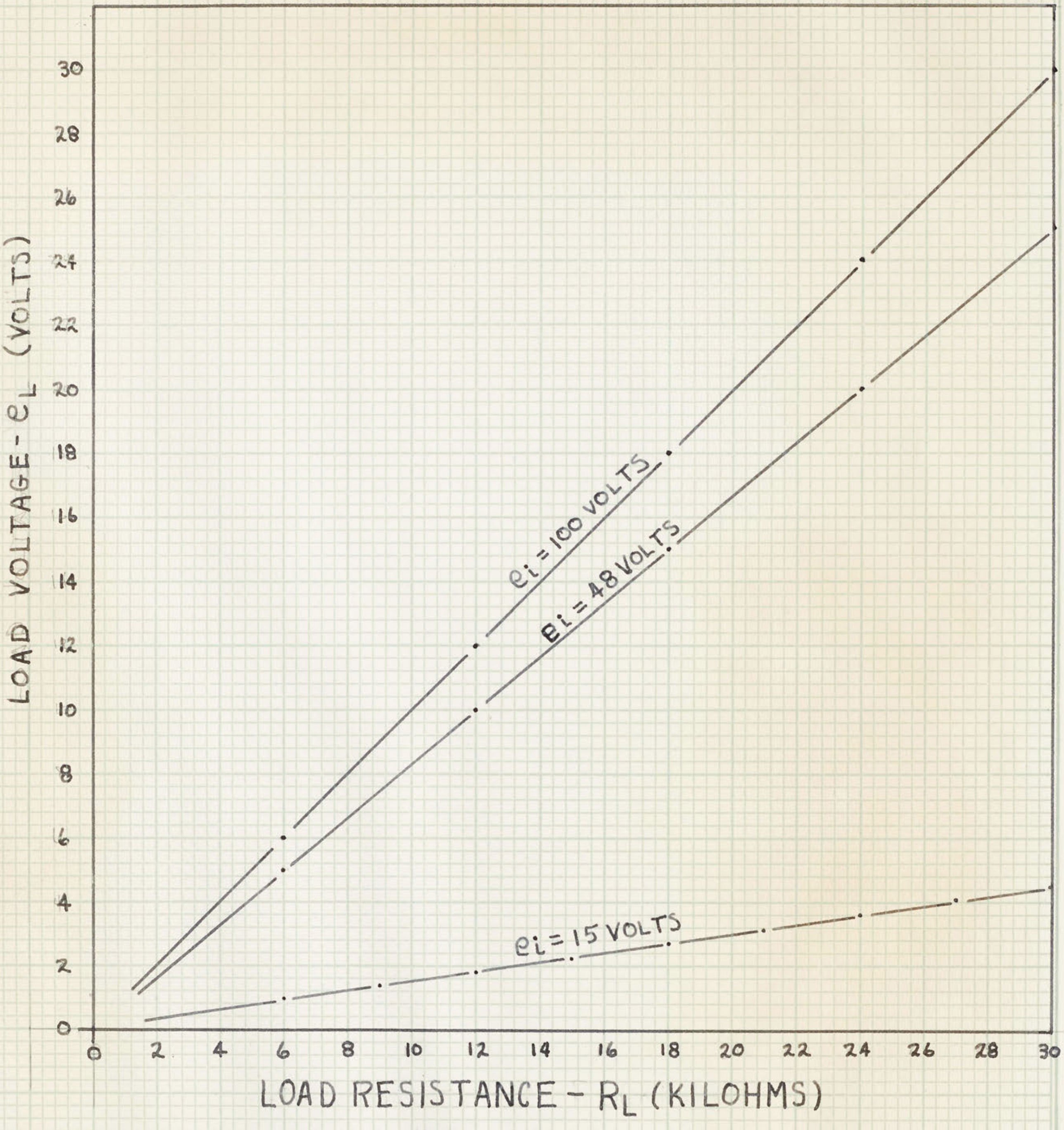

FIGURE 14.

LOAD VOLTAGE Vs LOAD RESISTANCE FOR CURRENT GENERATOR OF FIGURE C-3.

E. INTEGRATOR

The integrator presents somewhat of a design problem because of the operating times involved. The minimum time constant possible for the network is of the order of four seconds as discussed in the section on scanning frequency. The operating time of the simulator should be at least one hundred times this in order to give the network time to respond to information fedback from the integrator. This requires an operating time of 400 seconds. Because an integrator is required at every node in the slow group network it has to be simple and cheap to build and easy to operate. Also an accuracy of the order of one to two percent in the output is desired.

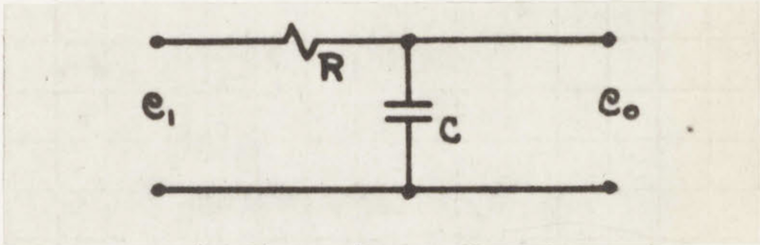

FIGURE 15.

The simplest type of integrator is the RC series circuit as discussed in Korn and Korn (12). and illustrated in figure 15. The percentage error ϵ or ratio of the difference between the response of the RC circuit and an ideal integrator of the same gain divided by the response of the ideal integrator is given by $\epsilon \leq \frac{T}{b}$ for a step input voltage. T is the time after the beginning of the step voltage and b is the time constant of the series circuit. In order to obtain an error of 2 percent or less in a computing time of 400 seconds- the time constant of the circuit must be b = 50 X 400/2 = 10,000 seconds. This value of time constant is out of the question using commercial electronics components. For a time constant equal to the computing time - which is near the limit that can be obtained with commercial components - the error can be shown to be approximately 36%. This amount of error is too great for this type of integrator to be of use in the proposed application.

The time constant of 10,000 seconds might be obtained with a mechanical device but the mechanism necessary would be too complicated to be practical for this application.

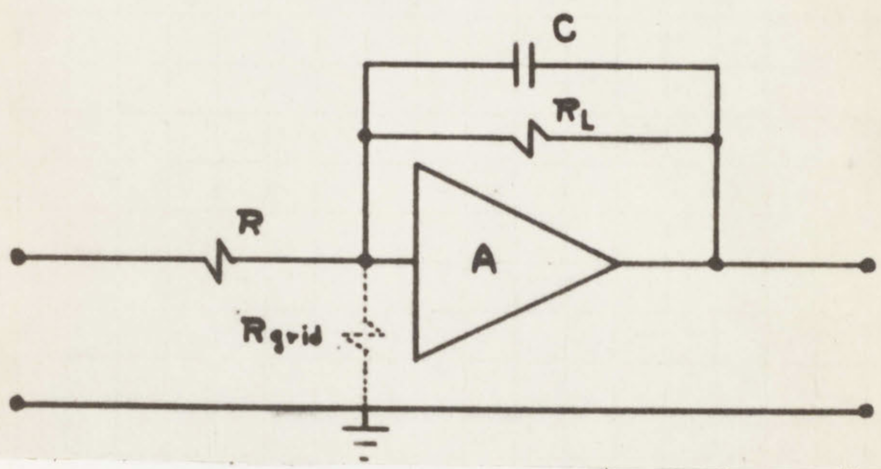

FIGURE 16

Other methods of integration involve the use of amplifiers with various feedback networks. The most generally used analog integrator is the parallel-feedback integrator shown in block diagram in figure 16. It consists of an integrating feedback network of R and C in conjunction with a DC amplifier of gain A. R_L constitutes the leakage resistance of the capacitor. Using the approximation that the grid current flowing in the amplifier input is negligible compared to the currents in the other resistances the nodal equation expressing Kirchoffs first law is written (14),

$$(1)\quad \left(\frac{e_o}{A} - e_o\right)\left(CP + \frac{1}{R_L}\right) + \left(\frac{e_o}{A} - e_i\right)\frac{1}{R} = 0$$

P is the Laplace operator

The transfer function obtained by manipulation of the above equation is

$$(2)\quad \frac{e_o}{e_i} = \frac{A}{(1-A)R/R_L + 1} \times \frac{1}{\frac{(1-A)RCP}{(1-A)R/R_L+1} + 1}$$

The time constant b and the "rate gain" $\frac{k}{b}$ are,

$$(3)\quad b = \frac{(1-A)RC}{(1-A)R/R_L + 1} \qquad (4)\quad \frac{k}{b} = \frac{A}{(1-A)RC}$$

Then by manipulation

$$(5)\quad \frac{e_o}{e_i} = \frac{1}{\left[\frac{(1-A)RC}{A}\right]P + \frac{1-A}{A}\frac{R}{R_L} + \frac{1}{A}}$$

The transfer function of the ideal integrator is

$$(6)\quad \frac{e_o}{e_i} = \frac{k}{bP}$$

The transfer function of equation 5 approaches that of the ideal integrator when $\frac{1-A}{A}\frac{R}{R_L} + \frac{1}{A} = 0$

This requires the A and R_L by very large. In practice, gains of A = 10^3 to 10^7 and capacitors with the highest R_L available are used. Because of the large R_L, required capacitor construction practice limits the values of C to the order of 1 μfd . Using a capacitor of 4 μfd. a resistor of 100 megohms is required for a time constant of 400 seconds. With this value of input resistance the analysis of the circuit no longer holds because of the approximation regarding the grid current. The fact that the circuit will not operate corrently with such a high input resistance coupled with the high cost of the low leakage capacitors necessary rules out the use of this type of integrator.

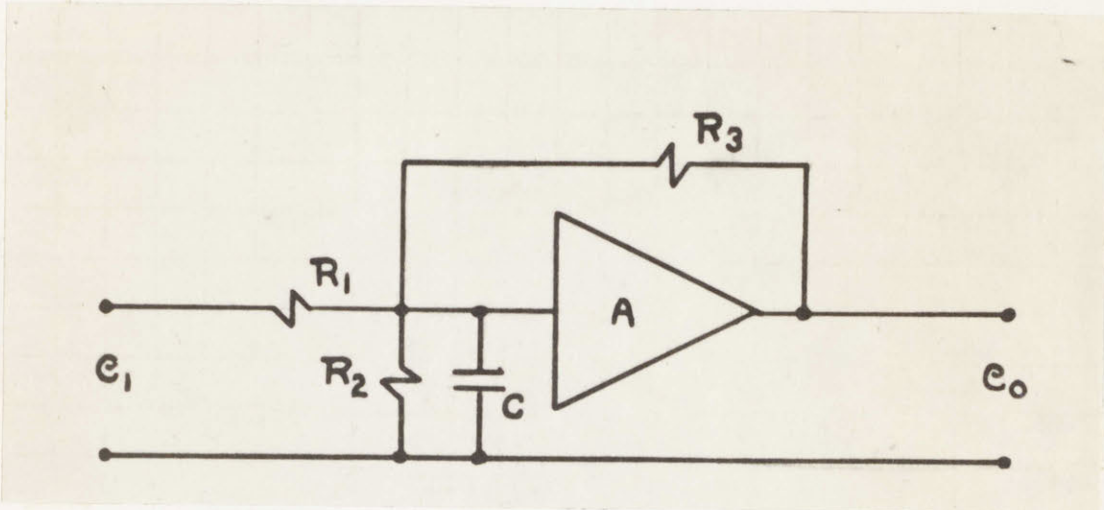

FIGURE 17

The circuit proposed for use is illustrated in block diagram in figure 17. The "bootstrap integrator" as it is called (15) is very similar to the current generator described in section IV-D. The circuit consists of a positive gain DC amplifier in conjunction with R_1 the input resistance, R_2 the capacitor leakage resistance, R_3 the feedback resistance and C the integrating capacitor. The nodal equation is written using the approximation that negligible grid current is drawn.

$$(7) \quad \frac{1}{R_1}\left(e_i - \frac{e_o}{A}\right) + \frac{1}{R_3}\left(e_o - \frac{e_o}{A}\right) = \frac{1}{R_2}\frac{e_o}{A} + \frac{Pe_oC}{A}$$

The transfer function may be written by manipulation of equation (7)

$$(8) \quad e_o\left[\frac{1}{AR_1} + \frac{1}{AR_2} + \frac{1}{AR_3} + \frac{PC}{A} - \frac{1}{R_3}\right] = \frac{e_i}{R_1}$$

$$(9) \quad \frac{e_o}{e_i} = \frac{A}{R_1CP + 1 + R_1/R_3 + R_1/R_2 - AR_1/R_3}$$

The transfer function for perfect integration will be obtained if $1 + R_1/R_3 + R_1/R_2 - AR_1/R_3 = 0$ or

(10)

$$A = \frac{R_3}{R_1} + \frac{R_3}{R_2} + 1$$

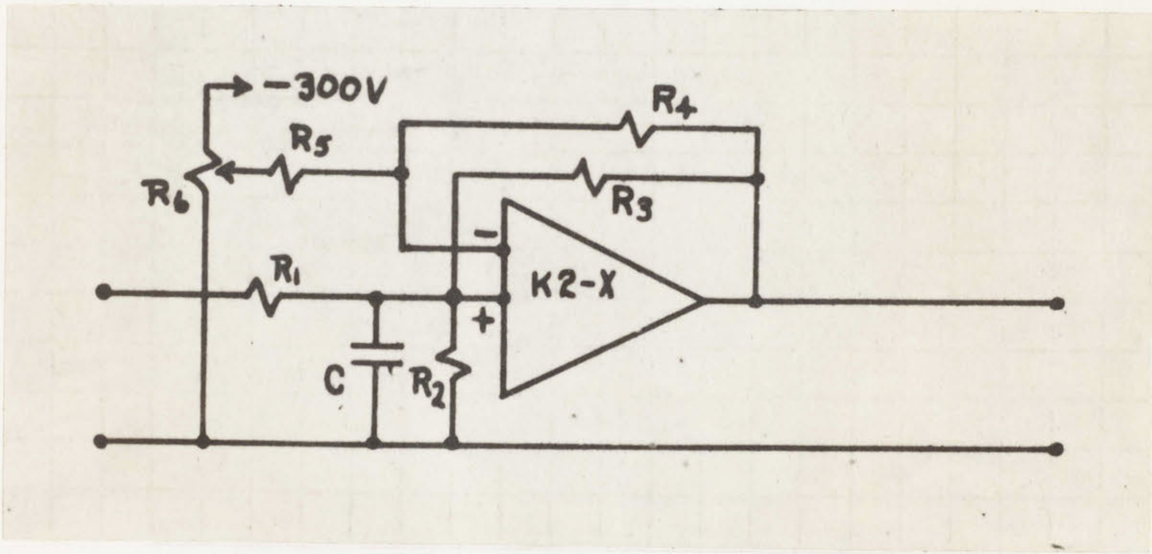

FIGURE 18.

The transfer function then becomes

(11) $$\frac{e_o}{e_i} = \frac{A}{R_1CP}$$

The advantages of this circuit are that the gain A required is low, the large value of R_1 required does not upset the analysis, and the required leakage resistance of the capacitor is not as high. Values or R_2 of the order of 100 Kilohms are allowed.

A schematic diagram of the proposed integrator is shown in figure 18.

The gain of the amplifier is given by

(12) $$A = \frac{R_4 + R_5}{R_5}$$

The values of the resistances used are R_2 = 100 megohm, R_2 = 200 kilohm and R_3 is to be 100 kilohm. C_4 is to be $4\mu fd$. The gain requirement then becomes by equation 10

(13) $$A = 1 + \frac{1}{1000} + \frac{1}{2} = 1.501 = \frac{R_4 + R_5}{R_5} \quad \therefore R_4 = 0.501 R_5$$

The output voltage for a step input voltage is given by equation 11 as $e_o = \frac{A}{R_1C}\int_0^t e_i dt = \frac{A}{R_1C} e_i t$

The maximum voltage possible from the slow resistor network is set by the current generators at 55V. Therefore the maximum value possible for the flux time integral is e_{imax} t_o where t_o is the operating time of the simulator. Using an operating time of 400 seconds equation 11 gives

(14) $$e_{o_{max}} = \frac{1.501 \times 55 \times 400}{400} = 82.5V$$

This is well below the 100V saturation voltage of the K2-X amplifier.

In practice R_2 will consist of the actual leakage resistance of the capacitor in parallel with a rheostat which allows the adjustment of the value of the parallel combination to the value of 200 kilohm. Resistances R_4 and R_5 are provided by a potentiometer and may be adjusted to match the R_1C time constant for each integrator. Thus the requirements on the tolerances of resistor R_1 and capacitor C are not quite as strict as if no adjustment were available.

F. FUNCTION GENERATOR

It is proposed that a function generator of the biased diode type GAP/R Model FFR be used. The operating speed required eliminates most of the types of function generators commonly used in analog computers leaving only the Cathode Ray Tube Photoformer (16) and the biased diode type (17). The biased diode type offers greater ease of operation and set up than the CRT type. Since this generator is available as a stock item it will not be discussed further.

G. MEASURING AND RECORDING APPARATUS

The measuring apparatus will be of two types. One will be a fast scanning system of moderate accuracy for monitoring the system during operation. The other will be a device of greater accuracy but of necessarily slower operation for taking data from the resistor networks.

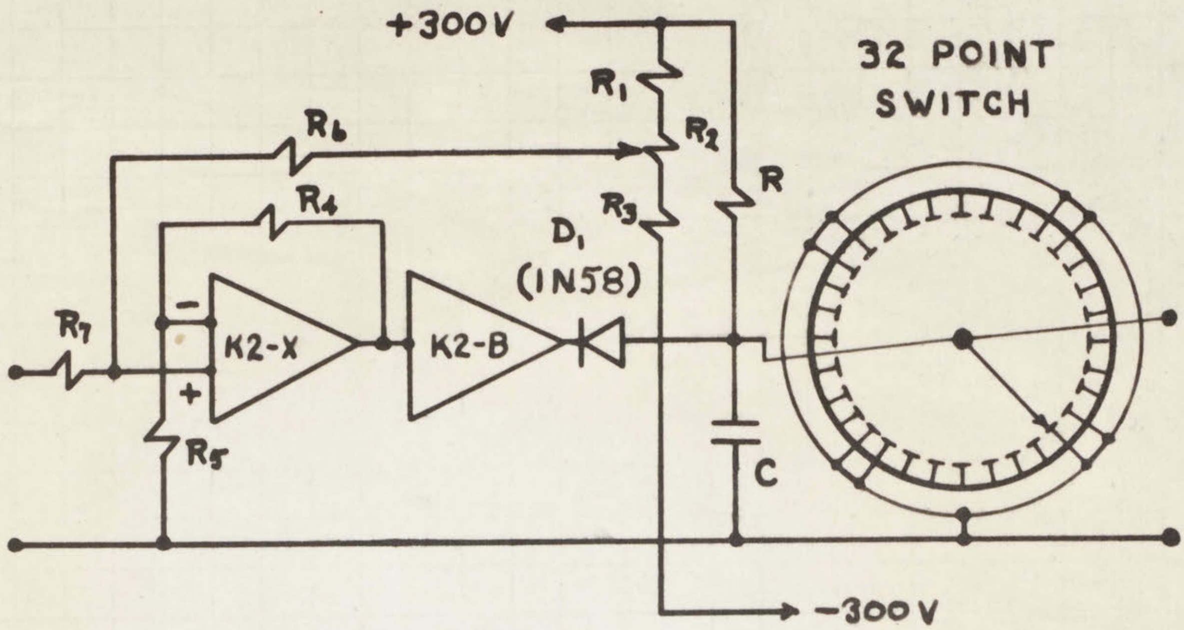

FIGURE 19.

A schematic diagram of the fast scan unit is shown in figure 19. The voltage from the network point being monitored is applied to the input terminal of a K2-X operational amplifier set up to have a gain of plus one. The output of the K2-X is applied to a K2-B amplifier in order to decrease the output impedance of the amplifiers. The capacitor C charges through resistor R toward the supply voltage (+300 volts). When the voltage on the capacitor equals the voltage from the K2-B amplifier the diode D_1 begins to conduct and shunts the current flowing through R to ground through R_L. This stops the charging of the capacitor causing the voltage across it to stabilize at some value slightly greater in magnitude than the voltage at the output of the K2-B amplifier. This excess voltage may be compensated for by means of the voltage divider consisting of R_1, R_2, and R_3 used to add a small negative voltage at the input to the K2-X amplifier. This voltage is of such a magnitude that it cancels the voltage drop due to the diode in the output circuit. When this is done the voltage on the capacitor equals the network voltage. The voltage at the capacitor is applied to vertical deflection terminal of an oscilloscope. In this way a vertical trace is generated on the oscilloscope the height of which is proportional to the network voltage being measured. The horizontal position of the trace is determined by the voltage from a voltage divider built as an integral part of the voltage scan switch.

The calibration of the unit may be changed by changing the gain of the K2-X amplifier. As an example to change the full scale deflector from 50 volts full scale as set up above to a value of 10 volts full scale the gain of the K2-X is increased from one to five by adjustment of R_1 and R_2.

VOLTAGE SCANNING SWITCH

Scanning rates of the order of 100 points per second are proposed in order that one complete network unit be scanned each second. Switches of the solid contact type are available which can operate at this speed. Four switch plates are necessary,a one-hundred contact plate for each of the two resistor networks and for the voltage divider used as a horizontal position indicator and one thirty-two contact plate for synchronizing the switch with the voltage measuring unit. The synchronization is indicated in figure 20.

The 32 contact plate is driven by a 30 rps synchronous motor. The three 100 contact plates are driven from this motor through a 25:1 gear reduction unit at 1.2 rps giving a scanning rate of 120 contacts per second.

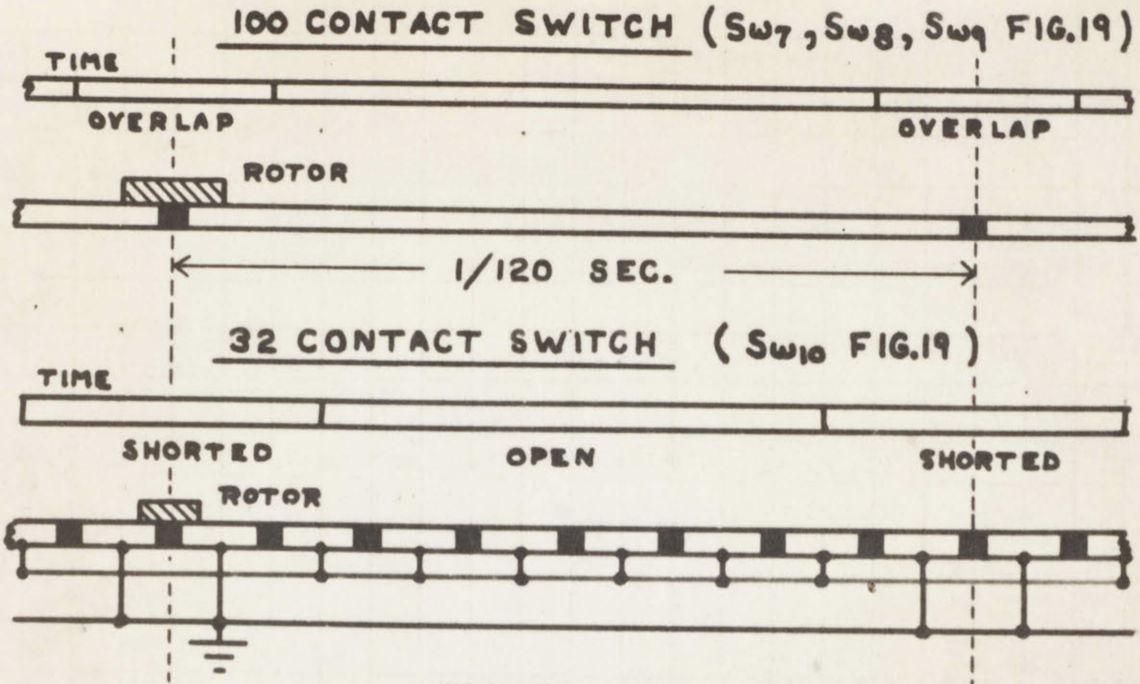

FIGURE 20

OSCILLOSCOPE

The oscilloscope to be used may be any of the large screen oscilloscopes currently on the market. One unit which might be used is the Model 1770 Monitor Oscilloscope by Electromic Incorporated. This unit uses a 17 inch cathode ray tube and is complete with vertical and horizontal amplifiers. No sweep circuitry is included but none is needed as the sweep voltages are generated externally.

HIGH ACCURACY MEASURING INSTRUMENTS

The higher accuracy measurements may be done with a digital voltmeter such as the Model DVA-500 by Electro-Instruments Company. Accuracies of the order of 0.01% are claimed by the manufacturer. The voltmeter would be connected to the network one point at a time as required by the operator.

PERMANENT RECORDING

Permanent records of the data obtained from the network can be obtained using a digital printout unit with the digital voltmeter described above. Units such as this are available from

Permanent records can be taken of the oscilloscope trace pattern with a camera.

CONTROL ROD SIMULATION

As mentioned in the section on boundary conditions - Section III-C - black control rods may be simulated by grounding the node points in the slow network corresponding to the space occupied by the rods. No current feed is made to the corresponding node points in the fast network as no fissions are produced in the control rod.

If the region occupied by the control rod is not completely black but is gray the absorption may be simulated by using resistances between the node point and ground. The value of the resistance to be used is computed from equations 11 using the proper scale factors.

A gray region may be due to a gray control rod or to partial occupation of the region by a black control rod. Partial occupation could be due to having only the tip of the rod in the region or due to having control rods small in relation to the region represented by the absorption and diffusion resistances. If the macroscopic absorption cross section of the region varies due to control rod motion then the resistance of the absorption resistor representing the properties of this region must be varied. In the reactor simulator system contemplated the control rod absorption resistances are varied in such a manner as to keep the system critical.

In the two dimensional simulator the control rod "motion" may be either in the plane of the simulator or perpendicular to it. For the case of rods in the plane of the simulator the absorption resistances are varied sequentially according to the motion of the tip of the rod. As the tip of the rod passes through a region of the reactor the resistor representing the absorption of this region alone is varied between the value for no control rod and the value for full control rod absorption. The other absorption resistances along the path of the control rod motion are left at either full or no control rod absorption. When either limit of the range of the resistance is reached the next resistor in the line of motion of the rod is used. This procedure is repeated until the rod is fully into or fully out of the reactor at which time no more control is possible with the rod.

For control rod motion perpendicular to the plane of the simulator the control rod absorption resistances are varied in accordance with the control rod gang scheme of the reactor. The limits of resistance used are determined from the control rod properties desired using equations 11 with the proper scale factors.

The variable resistances necessary are provided by a number of theostats arranged on the control rod simulator panel of the simulator. Patch cords are supplied for plugging the rheostats into the proper network node points. The absorption feed capacitor at each of these points is shorted out and the rheostat is placed in parallel with the network panel resistor.

The motion of the control rod rheostats is controlled by the operator in such a manner as to keep the simulator critical. An indication of the criticality of the system may be obtained from a voltmeter connected to a slow network node point. As long as the voltage remains constant - excluding the variation due to the feed current pulses - the simulator is critical. When the voltage decreases the resistance is increased and when the voltage increases the resistance is decreased. The rate of voltage change will determine the magnitude of the resistance change necessary to restore criticality.

V. ESTIMATE OF COST OF PROPOSED SIMULATOR

The construction of the simulator must be economically justifiable and in order to have some basis for determining this justification a cost estimate was made. The estimate unfortunately cannot be too accurate as little data is available on labor costs involved in the construction of such equipment. Also the author has little experience in this field on which to base an estimate. A rough guess will have to suffice. The equipment costs are obtainable and this information is given below. The estimate is for the cost of a one hundred point system.

Networks

Fast

320 Dual concentric-shaft potentiometers at $5.00	$ 1,600.00
100 5 capacitors, oil filled transmitting type at $5.00	500.00
100 Switches centralab PA-18 wafer on PA-300 index assembly at $2.00	200.00
100 Terminal Post-Superior 5-Way at $0.40	40.00

Slow

320 Dual concentric-shaft potentiometers at $5.00	1,600.00
200 5 capacitors, oil filled transmitting type at $5.00	1,000.00
100 Switches Centralab PA-18 wafer on PA-300 index assembly at $2.00	200.00
200 Terminal Post-Superior 5-Way at $0.40	80.00

Scanning Switches

6 Mercury Jet Scanning Switches Norwood Controls Corp. at $6.10	3,660.00
Plus 5 adapter plates at $21.00	105.00
Plus 1 motor at $90.00	90.00

Scanning Switches (Cont.)

1 4 plate Solid Contact Scan Switch 3-100 contact plates 1-32 contact plate-estimate	$ 600.00

Electronic Apparatus

2 Biased Diode Function Generators GAP/R Model FFR at $1,125.00	2,250.00
1 Duplex Multiplier Divider Unit GAP/R Model MU/DV at $750.00	750.00
100 Integrator units at $40.00	4,000.00

1 GAP/R Model K2-X amplifier	$28.00
1 4 μfd. capacitor-oil filled transmitting type	5.00
1 100K potentiometer	1.00
Miscellaneous hardware and resistors	6.00
	$40.00

5 GAP/R Model RK-200 power supplies at $355.00	1,655.00
3 Current generators at $140.00	420.00

2 GAP/R K2-X amplifier at $28.00	$ 56.00
2 GAP/R K2-B amplifier at $34.00	68.00
miscellaneous hardware and resistors	16.00
	$140.00

1 Voltage Ramp Generator at $80.00	80.00

1 GAP/R K2-X amplifier	$28.00
1 GAP/R K2-B amplifier	34.00
1 IN58A Crystal Diode	2.00
Miscellaneous hardware and resistors	16.00
	$80.00

1 17 inch Screen Cathode Ray Oscilloscope-estimate	1,000.00

Electronic Apparatus (Cont.)

1 Digital Voltmeter - estimate	$ 500.00
TOTAL	$19,130.00
Cost of panel for mounting fast and slow networks and other apparatus. Labor costs. Miscellaneous equipment and supplies.	6,000.00
TOTAL ESTIMATE	$25,130.00

APPENDIX A

COMPUTATION OF CONCENTRATIONS OF FISSION PRODUCTS IN U^{238} - U^{235} FUELED REACTOR AS A FUNCTION OF TIME AND FLUX LEVEL

In order to get some idea of the magnitudes and directions of the variations of fission products and fuel concentrations, a homogeneous fixed fuel reactor using a U^{235} - U^{238} mixture was taken as a sample problem. The differential equations describing the variations are presented and the analytic solutions given. These solutions are fairly cumbersome and not easily transformed to graphical form. A computer program for the analog computer solution is given and sample recordings of these solutions shown.

The isotopes to be considered in this study are U^{235}, U^{238}, U^{236}, Pu^{239}, Pu^{240}, Pu^{241} and fission products. Fission products fall into three major groups; 1) those with small cross sections and low branching ratios which do not saturate and which may be assumed to have a constant average cross section; 2) those which have fairly large cross sections and branching ratios and thus saturate at fairly large values of flux-time; and 3) those which have high cross sections, high branching ratios and a radioactive decay constant which produces saturation in a short time and where the level of saturation depends on the flux-level. Xenon-135 constitutes group 3, Samarium-149 group 2 and the remainder of the fission products are classed group 1.

The equations which describe the variations of these isotopes given below are taken from the notes on the forthcoming book by Benedict and Pigford, Chapter 3. The group 3 isotope Xenon-135 is not considered here as it does not contribute to the long term variations.

(1) U^{235} $$\frac{d\Sigma^{25}}{d\Theta} = -\sigma^{25}\Sigma^{25} \qquad \Theta = \int_0^t \phi_{(t)}\,dt$$

(2) U^{236} $$\frac{d\Sigma^{26}}{d\Theta} = \frac{\sigma^{26}\alpha^{25}\Sigma^{25}}{1+\alpha^{25}} - \sigma^{26}\Sigma^{26}$$

(3) U^{238} $$\frac{d\Sigma^{28}}{d\Theta} = -\sigma^{28}\left[\Sigma^{28} + (\eta^{25}\Sigma^{25} + \eta^{49}\Sigma^{49} + \eta^{41}\Sigma^{41})M\right]$$

$$M = \epsilon P_1(1-p) \quad , \quad P_1 = \exp(-B^2 T)$$

(4) Pu^{239} $$\frac{d\Sigma^{49}}{d\Theta} = \sigma^{49}\left[\Sigma^{28} + \eta^{25}\Sigma^{25}M + \Sigma^{49}(\eta^{49}M-1)\right]$$

(5) Pu^{240} $$\frac{d\Sigma^{40}}{d\Theta} = \sigma^{40}\left[\frac{\Sigma^{49}\alpha^{49}}{1+\alpha^{49}} - \Sigma^{40}\right]$$

(6) Pu^{241} $$\frac{d\Sigma^{41}}{d\Theta} = \sigma^{41}\left[\Sigma^{40} - \Sigma^{41}\right]$$

(7) FISSION PRODUCTS NON-SATURABLE

$$\frac{d\Sigma^{F}}{d\Theta} = \sigma^{F}\left[\frac{\Sigma^{25}}{1+\alpha^{25}} + \frac{\Sigma^{49}}{1+\alpha^{49}} + \frac{\Sigma^{41}}{1+\alpha^{41}} - \Sigma^{F}\right]$$

(8) FISSION PRODUCTS SATURABLE

$$\frac{d\Sigma_s}{d\Theta} = \beta\sigma^{s}\left[\frac{\Sigma^{25}}{1+\alpha^{25}} + \frac{\Sigma^{49}}{1+\alpha^{49}} + \frac{\Sigma^{41}}{1+\alpha^{41}}\right] - \sigma^{s}\Sigma^{S}$$

The solutions of equations (1) through (8) give the macroscopic cross sections for fuel and fission-products as a function of flux time. The absorption cross section Σ_{as} in equations (1) and (2) of section III-A may be considered to consist of Σ_{asc} the cross section of the cold clean reactor plus Σ_{asp} the change in cross section due to operation of the reactor.

Then

$$(9)\quad \Sigma_{asc} = \Sigma_o^{25} + \Sigma_o^{28} + \Sigma_o^{\text{MODERATOR}} + \Sigma_o^{\text{COOLANT}}$$

$$(10)\quad \Sigma_{asp} = \Sigma^{25} - \Sigma_o^{25} + \Sigma^{28} - \Sigma_o^{28} + \Sigma^{26} + \Sigma^{49} + \Sigma^{40} + \Sigma^{41} + \Sigma^{S} + \Sigma^{F}$$

$$(11)\quad \Sigma_{as} = \Sigma_{asc} + \Sigma_{asp}$$

This expression for Σ_{as} as a function of time is called $f_1(\theta)$.

Since $\Sigma_{as} = \Sigma_{asc} + \Sigma_{asp}$ then $\Sigma_{as}/\Sigma_{asc} = 1 + \Sigma_{asp}/\Sigma_{asc}$ and $a = \Sigma_{asp}/\Sigma_{asc}$. (12)

The source term for the fast group is given as $\eta\epsilon f\Sigma_{as}$. In addition to causing a change in Σ_{as} the operation of the reactor causes a change in ηf . This is due to the change in fuel type from pure U^{235} to a U^{235}, Pu^{239}, Pu^{241} mixture. The product ηf is equal to $\eta f = \nu\,\Sigma_{fs}/\Sigma_{as}$. By manipulation $\eta\epsilon f\Sigma_{as} = \nu\epsilon\Sigma_{fs}$. For a number (n) of fissionable isotopes $\eta\epsilon f\Sigma_{as} = \sum_{i=1}^{n}\epsilon\nu_i\Sigma_{fs_i}$. (13)

For the fuel system under consideration

$$(14)\quad \eta\epsilon f\Sigma_{as} = \epsilon\left[\frac{\Sigma^{25}}{1+\alpha^{25}} + \frac{\Sigma^{49}}{1+\alpha^{49}} + \frac{\Sigma^{41}}{1+\alpha^{41}}\right]$$

This expression for $\eta\epsilon f\Sigma_{as}$ as a function of time is called

$f_2(\theta)$. The functions $f_1(\theta)$ and $f_2(\theta)$ are applied to the circuit by the function generators F_1 and F_2.

A program for solving equations (1) through (8) and obtaining the functions $f_1(\theta)$ and $f_2(\theta)$ is given in figures (A-1a) and (A-1b). A Sodium-Graphite reactor was taken as a sample problem for use with this program. The nuclear properties of the reactor were taken from Benedict and Pigford (1). These are given in Table A-I. Cross section data for the various fuel isotopes and fission products were taken from Spinrad (21) and from Coryell and Sugarman (3). These appear in Table A-2. The computations of the various constants for use in the computer set up appear in Table A-3.

The computer program was set up on the REAC in the M.I.T. Servo-Mechanisms Laboratory and solutions run off. Some sample recordings of these solutions are given in figures (A-2a) through (A-2g). These are recordings for Σ^{25}, Σ^{49}, Σ^{40}, Σ^{41} and Σ^{F}. It will be noticed that figures (A-3e,f,g) cover shorter periods of flux-time than figures (A-3a,b,c,d). The solution for Σ^{F} is a rapidly rising function as shown in figure (A-3e) and saturates the computer in a short time. The recordings in figures (A-3a,b,c,d) were obtained with the sections for Σ^{S} and Σ^{F} disconnected.

More recordings were taken than appear here. Many of these were rendered valueless by the discovery of a mistake in wiring the program board of the computer. The mistake was discovered too late to repeat the computation and the data was discarded.

The initial conditions for equations (1) through (8) were set on the computer using $\Sigma_o^{25} = 100V$ and $\Sigma_o^{28}/\Sigma_o^{25} = 0.62$ so $\Sigma_o^{28} = 62V$. The macroscopic cross sections may be obtained from the recordings by using the scale factor $\Sigma_o^{25}/100$ so $\Sigma =$ recording voltage $\times\ \Sigma_o^{25}/100$. The time scale factor is $10^{21}\ n/cm^2\text{-sec}$. The flux time Θ is given by $\Theta = 10^{21}(n/cm^2\text{-sec})\ t$ where t is time after beginning of calculation obtained from recording.

The expression for Σ_{as} as a function of Θ given in equation 11 is applied to the resistor networks using the function generator F_1. F_1 may be set up to cover any total flux time by adjusting the time scale factor used. The integrator operating time is about 400 seconds. If a total flux-time of $4 \times 10^{21}\ n/cm^2$ is desired the scale factor becomes $1 \times 10^{19}\ n/cm^2\text{-sec}$. The integrator as set up in section IV-E goes through a maximum variation of 82.5V in 400 seconds. For a total flux time of $4 \times 10^{21}\ n/cm^2$ the voltage scale factor $4.85 \times 10^{19}\ n/cm^2\text{-Volt}$ is used to set up F_1 from equation 11.

The function generator F_2 is set up using equation 14 with the same time and voltage scale factors used for F_1.

XENON POISONING

Xenon with its moderately large cross section, high branching ratio and comparatively short half-life reaches saturation in the order of one day and must be considered separately from the other fission products. Because it saturates in such a comparatively short time it has little effect on the long term variation of flux distribution. The major effects on the flux distribution are over short periods of time following flux level changes and are flux level dependent as well as time dependent. The initial flux level distribution used in the long term variation studies should not be the cold clean distribution but should be the distribution obtained by considering the equilibrium Xenon concentrations over the reactor. Only the equilibrium concentrations will be considered here.

The production and decay scheme for Xenon-135 is given by

$$U^{235} \xrightarrow{n,f \ \gamma_2 = 0.003} Xe^{135}$$

$$U^{235} \xrightarrow{n,f \ \gamma_1 = 0.056} Te^{135} \xrightarrow{\beta^- \ 2 min} I^{135} \xrightarrow{\beta^- \ 6.7 hr} Xe^{135} \xrightarrow{\beta^- \ 9.2 hr.} Cs^{135}$$

$$I^{135} \xrightarrow{n,\gamma} I^{136} \qquad Xe^{135} \xrightarrow{n,\gamma} Xe^{136}$$

Since the Te^{135} half-period is so short the loss of this element due to neutron capture may be neglected. Thus I^{135} may be considered to be formed directly in the fission process with a branching ratio of 0.056.

The differential equations describing the rates of formation of Xenon and Iodine are

$$(15) \quad \frac{dI}{dt} = - I (\lambda_I + \sigma_I \Phi) + \gamma_1 \Sigma_f \Phi$$

$$(16) \quad \frac{dX}{dt} = - X (\lambda_X + \sigma_X \Phi) + I \lambda_I + \gamma_2 \Sigma_f \Phi$$

I and X are the concentrations per cubic centimeter of Iodine and Xenon respectively. γ_1 and γ_2 are the branching ratios and σ_I and σ_X are the cross sections in cm^{-2} of Iodine and Xenon. Φ is the flux level in the reactor and Σ_f is the macroscopic fission cross section of the fuel.

The solution to these equations for the concentration of Xenon is given by

(17)

$$X = X_0\left\{1-\exp\left[-(\lambda_X+\sigma_X\phi)t\right]\right\}+\frac{X_0\gamma_1(\lambda_X+\sigma_X\phi)}{(\lambda_X-\lambda_I+\sigma_X\phi)(\gamma_1+\gamma_2)}\left[\exp\left[-(\lambda_X+\sigma_X\phi)t\right]-\exp(-\lambda_I t)\right]$$

where X_0 is the equilibrium concentration equal to

(18) $$X_0 = \frac{\Sigma_f\,\phi\,(\gamma_1+\gamma_2)}{\lambda_X+\sigma_X\phi}$$

(19) $$\Sigma^{X_0}/\Sigma_f = \frac{\sigma_X\,\phi\,(\gamma_1+\gamma_2)}{\lambda_X+\sigma_X\phi}$$

Substitution of the numerical values for the constants gives

(20) $$\Sigma^{X_0}/\Sigma_f = 0.059\left[\frac{3.5\times10^{-18}\phi}{3.5\times10^{-18}\phi+2.9\times10^{-5}}\right]$$

The ratio Σ^{X_0}/Σ_f is defined as the poisoning. The maximum equilibrium poisoning is given by equation 20 as $\left(\Sigma^{X_0}/\Sigma_f\right)_{max} = 0.059$. Equation 20 may be rewritten then as

(21) $$\Sigma^{X_0}/\Sigma_f = \left(\Sigma^{X_0}/\Sigma_f\right)_{max}\left[\frac{3.5\times10^{-18}\phi}{3.5\times10^{-18}\phi+2.9\times10^{-5}}\right]$$

A plot of equation 21 is given in figure A-3.

Because the effects of the Xenon occurs in very short periods following startup the fuel may be considered to be only U^{235} and equation 21 becomes

(22) $$\Sigma^{X_0}/\Sigma_f = \frac{\Sigma^{X_0}}{\Sigma_0^{25}/1+\alpha^{25}} = \frac{(1+\alpha^{25})\Sigma^{X_0}}{\Sigma_0^{25}}$$

$$(23) \quad \Sigma^{X_0} / \Sigma_0^{25} = \frac{0.059}{1+\alpha^{25}} \left[\frac{3.5\times10^{-18}\phi}{3.5\times10^{-18}\phi + 2.9\times10^{-5}} \right]$$

This expression may be used in calculating Σ_{as} as a function of flux level for use in the simulator equation 11 with $\Sigma^{49} = \Sigma^{40} = \Sigma^{41} = \Sigma^{S} = \Sigma^{F} = 0$. Then instead of feeding the signal from the integrator into the function generator F_1 as in figure 9, Section IV, the voltage taken from the slow network would be used. The function generator F_2 and the integrator would not be used. The gain of the current amplifier M_2 would be constant at the value computed from the fuel properties.

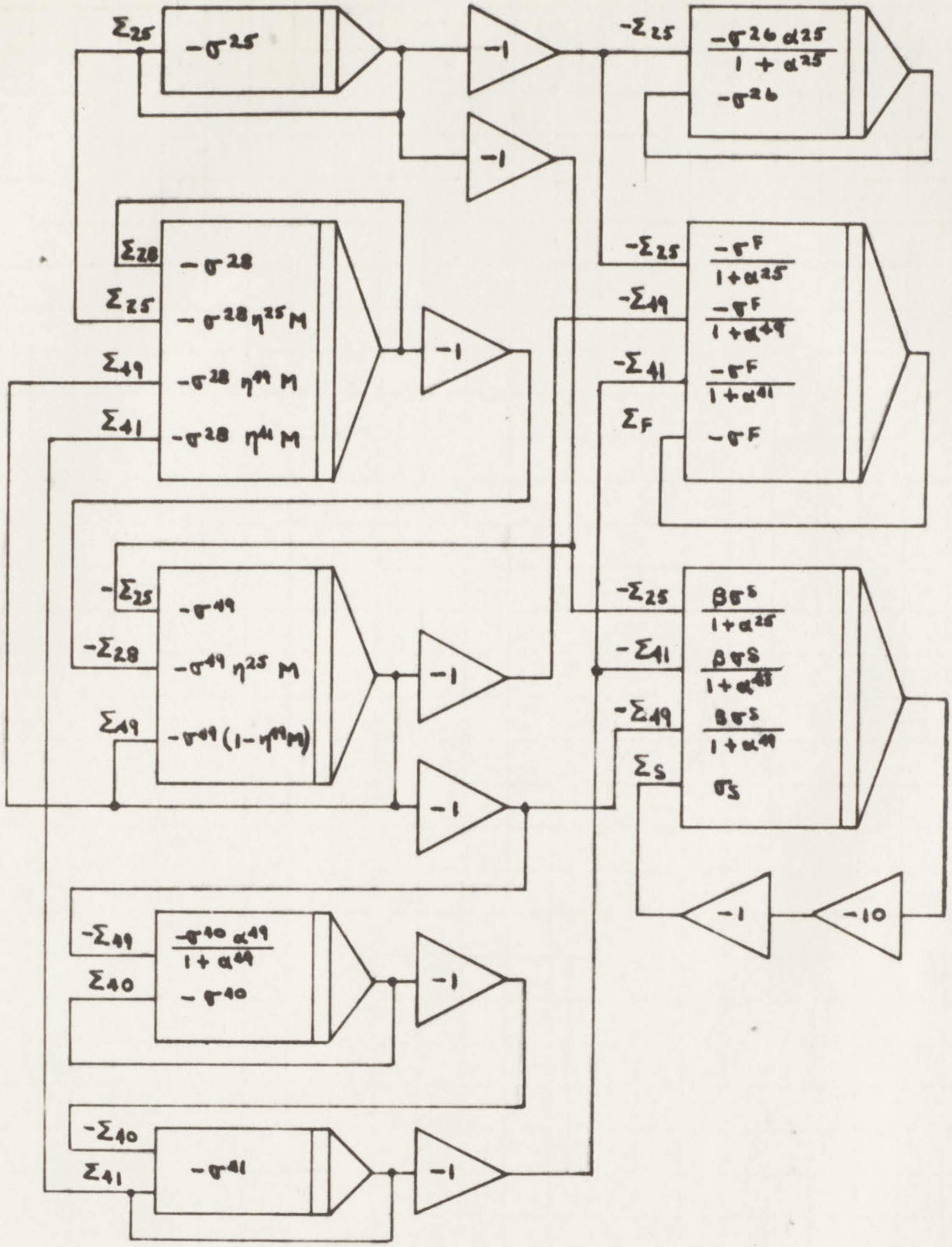

Σ_{25}
$-\sigma^{25}$
-1
$-\Sigma_{25}$
$\frac{-\sigma^{26}\alpha^{25}}{1+\alpha^{25}}$
$-\sigma^{26}$
Σ_{28}
$-\sigma^{28}$
$-\sigma^{28}\eta^{25}M$
Σ_{49}
$-\sigma^{28}\eta^{49}M$
Σ_{41}
$-\sigma^{28}\eta^{41}M$
$-\Sigma_{49}$
$-\Sigma_{41}$
$\frac{-\sigma^F}{1+\alpha^{25}}$
$\frac{-\sigma^F}{1+\alpha^{49}}$
$\frac{-\sigma^F}{1+\alpha^{41}}$
Σ_F
$-\sigma^F$
$-\Sigma_{28}$
$-\sigma^{49}$
$-\sigma^{49}\eta^{25}M$
$-\sigma^{49}(1-\eta^{49}M)$
$\frac{\beta\sigma^S}{1+\alpha^{25}}$
$\frac{\beta\sigma^S}{1+\alpha^{41}}$
$\frac{\beta\sigma^S}{1+\alpha^{49}}$
Σ_S
σ_S
-10
$\frac{-\sigma^{40}\alpha^{49}}{1+\alpha^{49}}$
Σ_{40}
$-\sigma^{40}$
$-\Sigma_{40}$
$-\sigma^{41}$

FIGURE A-1

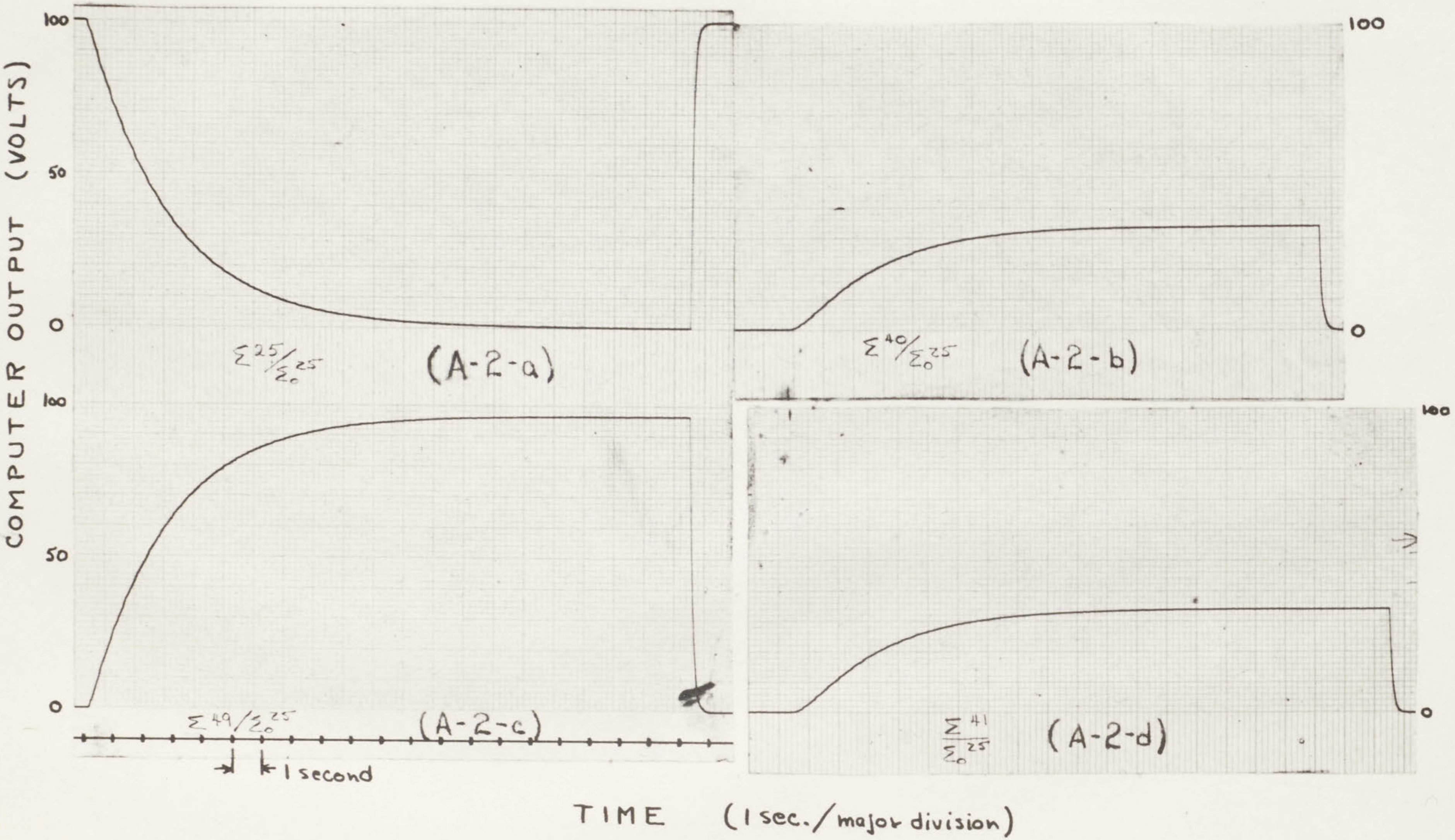

100
50
0
COMPUTER OUTPUT (VOLTS)
(A-2-a)
(A-2-b)
(A-2-c)
(A-2-d)
1 second
TIME (1 sec./major division)

FIGURE A-2

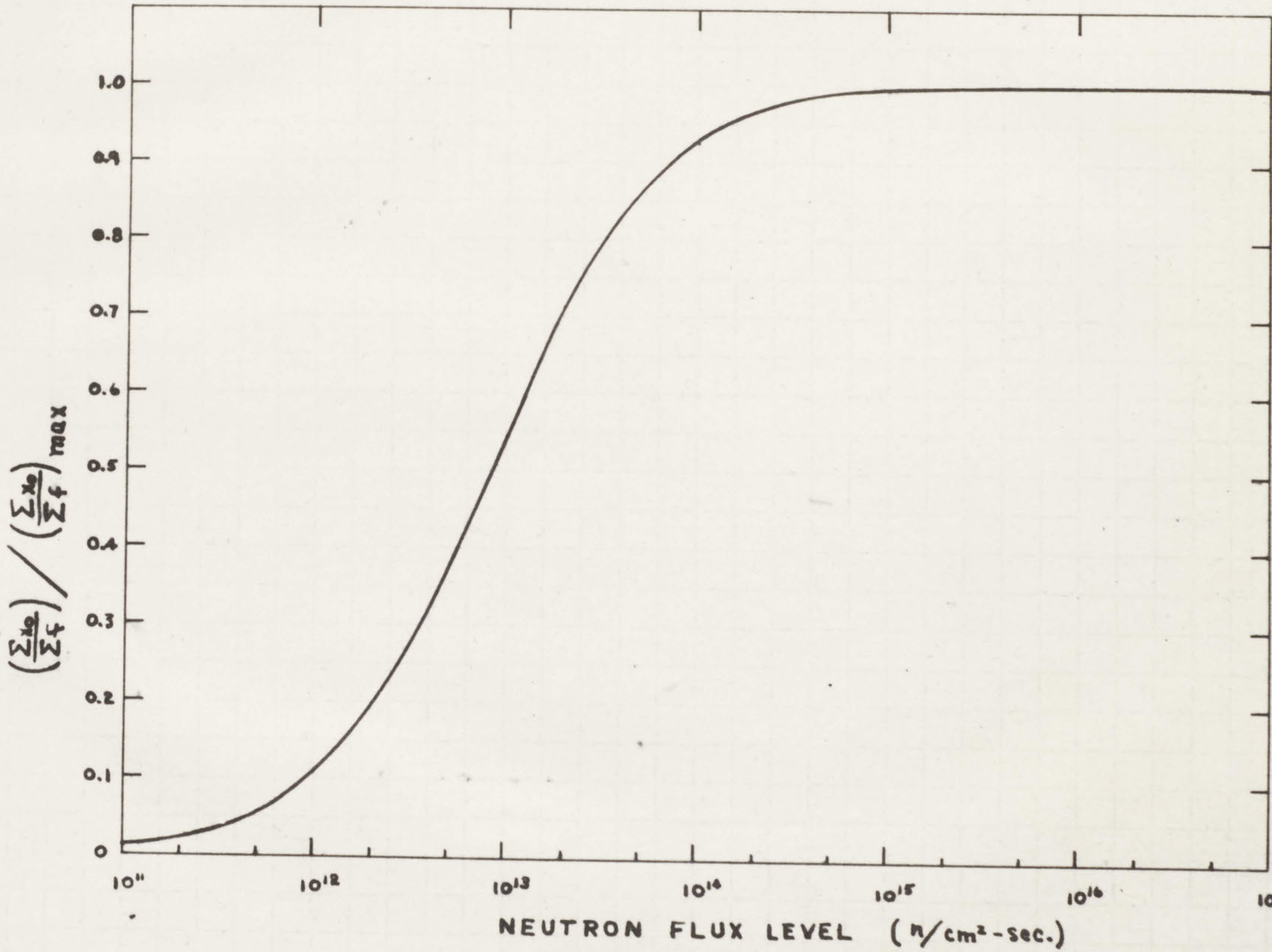

1.0
0.9
0.8
0.7
0.6
0.5
0.4
0.3
0.2
0.1
0
$\left(\frac{\Sigma_{xe}}{\Sigma_f}\right) \Big/ \left(\frac{\Sigma_{xe}}{\Sigma_f}\right)_{max}$
10^{11}
10^{12}
10^{13}
10^{14}
10^{15}
10^{16}
10^{17}
NEUTRON FLUX LEVEL (n/cm² - sec.)

FIGURE A-3

TABLE A-1

TYPICAL PROPERTIES OF SODIUM-GRAPHITE-URANIUM POWER REACTOR

Fuel	Uranium, slightly enriched
Enrichment, atom per cent U-235 in uranium	1.00
Reactor Geometry	Circular cylinder
Height, ft.	13.1
Radius, ft.	7.1
Fuel Element	Zirconium-clad tube of uranium metal, 0.820 in. ID, 1.54 in. OD
Moderator	Graphite, pierced with holes for process tubes
Process Tube (Contains fuel element and sodium coolant)	Zirconium tube, 2.00 in. ID, 0.040 in. thick
Lattice Arrangement of Process Tubes	Spaced 7.0 in. on triangular centers
Number of Process Tubes	536
Total Mass of Uranium, kgm.	31,500
Total Mass of U-235, kgm.	308
Average Temperature (at which neutrons are thermalized)	400°C
Fast Fission Factor,	1.027
Fission-to-Resonance Non-Leakage Probability, P_1	0.964
Fission-to-Thermal Non-Leakage Probability, P_{th}	0.954
Resonance Escape Probability, p	0.800

TABLE A-2

EFFECTIVE THERMAL-NEUTRON PROPERTIES OF NUCLIDES FOR IRRADIATION CALCULATIONS

	Total Absorption Cross Section (barns)	Fission Neutrons per Absorption	Ratio of Capture to Fission Cross Section
U-235	378	2.08	0.184
U-236	6.6	0	
U-238	1.64	0	
Pu-239	1660	1.83	0.5734
Pu-240	2249	0	
Pu-241	1409	2.14	0.3454
Pu-242	19.75	0	

TABLE A-3

COMPUTATION OF CONSTANTS FOR USE ON COMPUTER

$M = \epsilon P_1 (1-p) = 1.03 \times .954 \times .200 = 0.1965$

$\sigma^{28} \eta^{25} M = 1.64 \times 2.08 \times .196 = .669$

$\sigma^{28} \eta^{49} M = 1.64 \times 1.83 \times .196 = .588$

$\sigma^{28} \eta^{41} M = 1.64 \times 2.14 \times .196 = .688$

$\sigma^{49} \eta^{25} M = 1660 \times 2.08 \times .196 = 676$

$\sigma^{49} (1 - \eta^{49} M) = 1660 \times (1 - 1.83 \times .196) = 1065$

$$\frac{\sigma^{40} \alpha^{49}}{1+\alpha^{49}} = \frac{2249 \times .573}{1.573} = 820$$

$$\frac{\sigma^{26} \alpha^{25}}{1+\alpha^{25}} = \frac{6.6 \times .184}{1.184} = 1.02$$

$$\frac{\sigma_F}{1+\alpha^{25}} = \frac{80}{1.184} = 67.5$$

$$\frac{\sigma^F}{1+\alpha^{49}} = \frac{80}{1.573} = 50.8$$

$$\frac{\sigma_F}{1+\alpha^{41}} = \frac{80}{1.345} = 59.5$$

$$\frac{\beta \sigma^S}{1+\alpha^{25}} = \frac{7.64 \times 10^2}{1.184} = 645$$

$$\frac{\beta \sigma^S}{1+\alpha^{49}} = \frac{7.64 \times 10^2}{1.573} = 485$$

$$\frac{\beta \sigma^S}{1+\alpha^{41}} = \frac{7.64 \times 10^2}{1.345} = 568$$

APPENDIX B

ANALYSIS OF CURRENT GENERATOR

In order to follow the analysis of the current generator the reader should be familiar with the principles of the operational amplifier as used in computer applications. A short resume is given of these principles followed by the analysis of the current generator.

The operational amplifier consists of a high gain (10^3-10^7) direct-current amplifier of very high input impedance (10^8-10^9 ohms) designed to have stable gain and very low operating point drift. By the use of proper feedback networks various mathematical operations may be performed with the amplifier. The simplest operation possible is multiplication by a constant. A simplified diagram of the circuitry required is shown in figure C-1. The amplifier is designated by a triangle whose base is the input and whose apex is the output end.

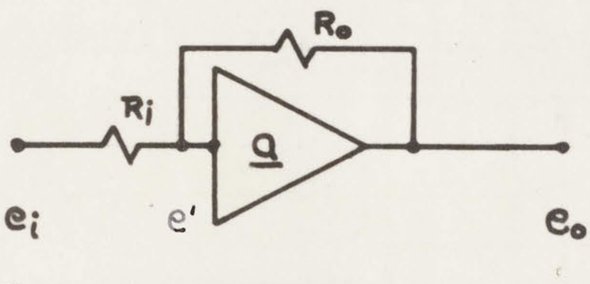

FIGURE C-1.

Voltage e_i is input voltage to computer unit terminals, e_o is voltage at output terminals. R_i is input resistance and R_o is feedback resistance.

Voltages e' and e_o are related by the gain of the amplifier a. Thus $e_o = -ae'$ or $e' = -\frac{e_o}{a}$. With a very high gain the voltage e' is not very much different from zero for a finite output e_o. According to Kirchoff's law the sum of all the currents flowing into the junction point at e' must be zero. Thus

$$(1) \quad \frac{e_i - e'}{R_i} + \frac{e_o - e'}{R_o} = 0$$

$$(2) \quad e' = -\frac{e_o}{a}$$

$$(3) \quad \frac{e_i + \frac{e_o}{a}}{R_i} + \frac{e_o + \frac{e_o}{a}}{R_o} = 0$$

$$(4) \quad e_o = \frac{-a e_i}{1 + R_i/R_o (1+a)}$$

if $a \gg 1$ then $(1+a)\frac{R_i}{R_o} \gg 1$, $1+a \simeq a$ and

$$(5) \quad e_o \simeq \frac{-a e_i}{a R_i/R_o} = -e_i \frac{R_o}{R_i}$$

The requirements for this analysis to be true are that a 1 and that the grid current of the amplifier be very small compared to the currents in resistors R_1 and R_o. In most commercial computer amplifiers these requirements are met to the extent that errors due to grid currents are completely negligible compared to errors in resistance values.

Summation may be accomplished by adding inputs as shown in figure C-2.

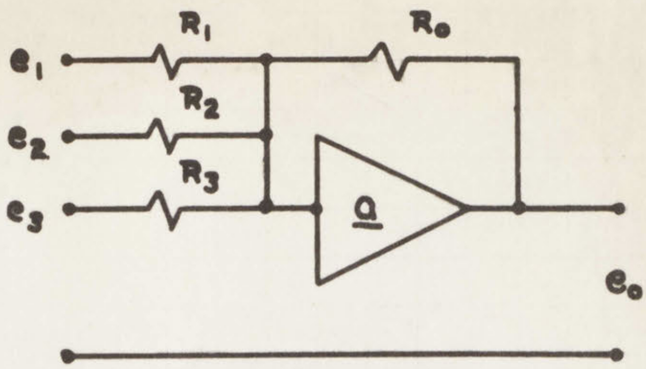

FIGURE C-2

$$(6) \qquad e_o = \frac{-\frac{a e_1}{R_1} - \frac{a e_2}{R_2} - \frac{a e_3}{R_3}}{\frac{1}{R_1} + \frac{1}{R_2} + \frac{1}{R_3} + \frac{1}{R_o}(1+a)}$$

if $a \gg 1$ then $1+a \simeq a$ and

(7)

$$e_o = -\left[\frac{R_o}{R_1} e_1 + \frac{R_o}{R_2} e_2 + \frac{R_o}{R_3} e_3\right]$$

Thus the process of summation has been performed and it is apparent that each voltage e_i could have been multiplied by a constant also. More detailed explanations of the use of operational amplifiers may be found in various texts on analog computers (Korn and Korn (13), Johnson (10), Soroka (20)).

A current generator is a device which produces a current at its output which does not vary with output voltage or resistance. The generator proposed for use in the reactor simulator makes use of the "bootstrap" type circuit described by Puckle (19). Consider the circuit shown in figure C-3.

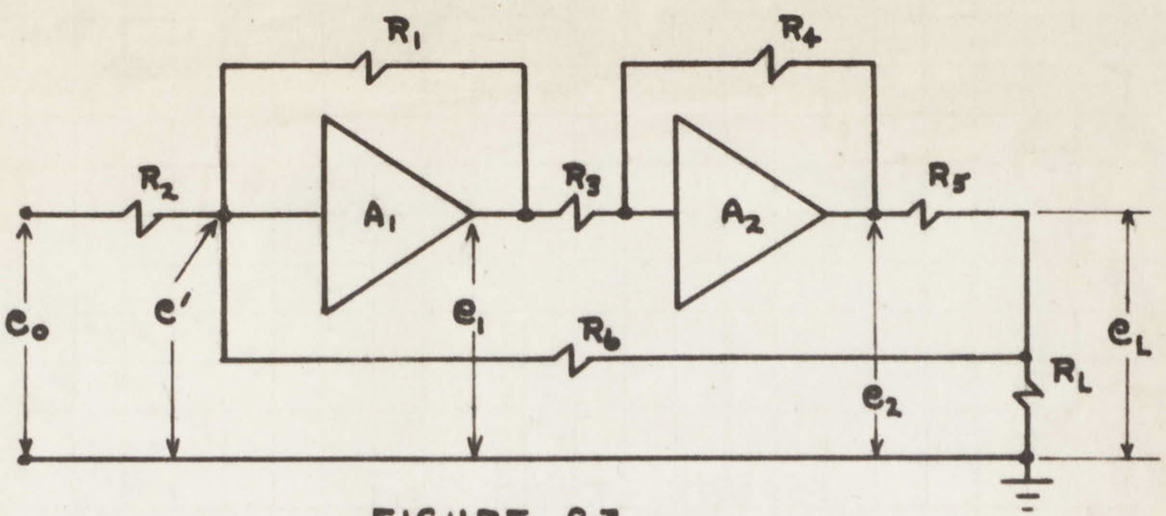

FIGURE C-3

The voltage relationships for voltages e_1, e_2, and e_L may be written as follows

(8) $$e_L = \frac{e_2 R_L}{R_5 + R_L}$$ (8a) $$i_L = \frac{e_2}{R_5 + R_L}$$

(9) $$e_1 = -\left[e_0 \frac{R_1}{R_2} + e_L \frac{R_1}{R_6} \right]$$

(10) $$e_2 = -\frac{R_4}{R_3} e_1 = \frac{R_4}{R_3}\left[e_0 \frac{R_1}{R_2} + e_L \frac{R_1}{R_6} \right] = \frac{R_4}{R_3}\left[e_0 \frac{R_1}{R_2} + e_2 \frac{R_1 R_L}{R_6 (R_5 + R_L)} \right]$$

Simplifying 10

(11) $$e_2 = e_0 \frac{R_1 R_3 R_4 R_6 (R_5 + R_L)}{R_2 R_3 \left[R_3 R_6 (R_5 + R_L) - R_1 R_4 R_L \right]}$$

Substituting 10 into 8a

(12) $$i_L = e_0 \frac{R_1 R_4 R_6}{R_2 (R_3 R_5 R_6 + R_3 R_6 R_L - R_1 R_4 R_L)}$$

if $R_3 = R_4$ and $R_1 = R_6$ 12 becomes

(13) $$i_L = \frac{e_0 R_1}{R_5 R_2}$$

If R_1/R_2 is called A

(14)

$$i_L = \frac{Ae_o}{R_5}$$

Thus the circuit satisfies the requirements of the current generator in that the current expressed by equation 13 does not depend on either R_L or e_L. This will be true only if the operating limits of the amplifiers are not exceeded. In switching the current generator units, care must be taken to see that the output is never open circuited while the input is connected. The infinite resistance at the output will cause the amplifier to saturate.

Figure 13 in Section IV-D shows the circuit described above using GAP/R Model K2-X operational amplifiers for A_1 and A_2. The GAP/R Model K2-B amplifiers are used to provide greater output currents than are available from the K2-X units. The analysis of the current generator is not changed by the addition of these units. They may be considered to be part of A_2 along with the K2-X amplifier. More than two K2-B units may be used if the current requirement is increased.

APPENDIX C

LITERATURE CITATIONS

(1) Benedict, M. and Pigford, T. H., Notes on Fuel Cycles in Thermal Nuclear Reactors used in course N-23 at M.I.T. (1957).

(2) Clark, M. H., Personal communication in course N-22 at M.I.T. (1957).

(3) Coryell, C. D. and Sugarman, N., Eds., Radio Chemical Studies; The Fission Products, National Nuclear Energy Series, Div. IV, Vol. 9, McGraw-Hill Book Co., New York, 1951.

(4) Elmore, W. C. and Sands, M., "Electronics - National Nuclear Energy Series V-1", pp 71-75, New York, McGraw-Hill Book Co., Inc., 1949.

(5) Glasstone, S. and Edlund, M. C., "The Elements of Nuclear Reactor Theory", pp. 238-247, Princeton, New Jersey, D. Van Nostrand Co., Inc., 1952.

(6) Habetler, G. J., "One Space Dimensional Multigroup", for the IBM 650, Part I, Equations KAPL-1415, Schenectady, New York, (1955).

(7) Harrer, J. M., "Nuclear Reactor Simulator", ANL-4294, Oak Ridge, Tennessee, Technical Information Extension, (1949).

(8) Honeck, H. C. and Ott, D. G., Chemical Engineering Progress Symposium Series No. 12, Part II, Vol. 50, (1954).

(9) Howe, R. M. and Haneman, T., Proceeding of IRE XLI, pp 1497-1508, (1953).

(10) Johnson, C. L., "Analog Computer Techniques" New York McGraw-Hill Book Co., Inc., 1956.

(11) Karplus, W. J., British Journal of Applied Physics 6, (1955).

(12) Korn, G. A. and Korn, T. M., "Electronic Analog Computers", pp 125, New York, McGraw-Hill Book Co., Inc., 1952.

(13) Ibid, pp 116-157.

(14) Ibid, pp 138-145.

APPENDIX C

LITERATURE CITATIONS (CONT'D)

(15) Ibid., pp. 137-138.

(16) Ibid., pp. 247-251

(17) Ibid., pp. 275-279.

(18) Kron, G., Electrical Engineering LXVIII, pp. 672-684 (1948).

(19) Puckle, O. S., "Time Bases", pp. 135-137, New York, John Wiley and Sons (1951).

(20) Soroka, W. W., "Analog Methods in Computation and Simulation", pp. 41-96, New York, McGraw-Hill Book Company, Inc. (1954).

(21) Spinrad, B. I., Carter, J. C., Eggler, C., "Record of Conference on Peaceful Uses of Atomic Energy, Volume 5", pp. 125-133.

(22) Spooner, R. B., Nucleonics 12 No. 4, pp. 36-39 (April, 1954).

(23) Varga, R. S., "Numerical Solution of the Two-Group Diffusion Equations in X-Y Geometry", WAPD 159 (1956).